

“ $L = R$ ” – $U(1)_R$ as the Origin of Leptonic ‘RPV’

Claudia Frugiuele^{†,c}, Thomas Grégoire[†], Piyush Kumar^{*,§}, Eduardo Pontón^{*}

[†]*Ottawa-Carleton Institute for Physics
Department of Physics, Carleton University
1125 Colonel By Drive, Ottawa, K1S 5B6 Canada*

^c*Theoretical Physics Department
Fermilab
P.O. Box 500, Batavia, IL 60510 USA*

^{*}*Department of Physics & ISCAP
538 W 120th street
Columbia University, New York, NY 10027 USA*

[§]*Department of Physics
Yale University, New Haven, CT 06520 USA*

Abstract

A classification of phenomenologically interesting supersymmetric extensions of the Standard-Model with a $U(1)_R$ symmetry is presented. Some of these are consistent with subsets of leptonic or baryonic “R-parity violating” (RPV) operators, thereby providing a natural motivation for them. We then focus on a particular class of models in which the $U(1)_R$ symmetry coincides with lepton number when restricted to the SM sector. In this case, the extension of lepton number to the superpartners is “non-standard”, implying, in particular, the existence of the leptonic RPV operators LLE^c and LQD^c , and a vacuum structure where one of the left-handed sneutrinos acquires a significant vacuum-expectation-value, while not being constrained by neutrino mass bounds. The model can be naturally consistent with bounds from electroweak precision measurements and flavor-changing processes. It can also easily accommodate the recently measured Higgs mass due to the existence of a scalar triplet that couples to the Higgs with an order one coupling, with only moderate fine-tuning. The phenomenology is rather rich and distinctive, with features such as heavy-but-natural Dirac gauginos, relaxed bounds on squarks, resonant slepton/sneutrino production, lepto-quark signals, as well as an interesting connection to neutrino physics arising from R -breaking. The broad qualitative features are discussed in this paper, with a more detailed phenomenological study carried out in a companion paper [1].

September 23, 2018

Contents

1	Introduction	2
2	Classification of R-symmetric Models	4
2.1	Supersymmetry Breaking	6
2.2	R -breaking	8
3	Characteristic Features of the Model with $R = R_1$	9
4	The Fermionic Electroweak Sector	11
4.1	Charginos & Charged Leptons	11
4.2	Neutralinos & Neutrinos	11
5	Indirect Constraints	12
5.1	Constraints on the sneutrino vev $v_{(a)}$ ($\tan\beta$)	12
5.2	Constraints on λ and λ' couplings	14
6	The Scalar Electroweak Sector	17
6.1	The ~ 125 GeV Eigenstate	19
7	Phenomenology	21
7.1	Summary of Bounds from Existing Searches	23
7.2	Resonant Slepton/Sneutrino Production	24
7.3	Lepto-quark (LQ) Signals – R -symmetry at the TeV Scale	25
7.3.1	Special Cases	28
7.4	LHC Signals of a Large Sneutrino vev	29
7.5	Distinguishing from Other Models	30
7.6	The Case “ $B = R$ ”	31
8	Dark Matter	32
9	Conclusions and Future Directions	33
A	R-breaking Operators	35
B	A Flavor Ansatz	36
C	Lower Bound on λ'_{i33} given the Observation of an LQ Signal	38

1 Introduction

We are extremely fortunate to live in a data-rich era of particle physics. The discovery of a Higgs-like particle [2, 3] is indeed a monumental achievement of the LHC. Measuring the properties of this particle in detail is now one of the most important experimental tasks. On the other hand, the mass of this particle (~ 125 GeV), as well as null results for beyond the Standard-Model (SM) physics so far, have started challenging our simple expectations for physics beyond the SM.¹ In particular, the Minimal Supersymmetric Standard Model (MSSM), which is the leading candidate for beyond-the-Standard Model (BSM) physics, is being significantly constrained. For example, the bounds on colored superpartners are well over a TeV in the “bulk” of parameter space, where pair production of squarks and/or gluinos is followed by decay into quarks or gluons and the lightest supersymmetric particle (LSP), giving rise to a jets plus \cancel{E}_T signature.

How can one interpret the Higgs-like discovery at ~ 125 GeV, and the null results for new physics so far? Our discussion will be within the supersymmetric paradigm for concreteness. The current data seems to suggest two rather different approaches to beyond-the-SM (BSM) physics. One viewpoint is that a Higgs near 125 GeV and the absence of superpartners so far, can be explained in the MSSM with heavy ($\sim 10 - 100$ TeV) scalars. These models are therefore *electroweak-tuned*. Models of this type can arise in some versions of [4, 5]. In fact, there exist top-down frameworks which predict heavy scalars in the 10-100 TeV range [6, 7] and, therefore, a Higgs mass near the observed value [8]; the *big* hierarchy problem of dynamically generating the (~ 10) TeV scale from the Planck scale is solved in such a framework, but a *little* hierarchy remains.

However, the other viewpoint is that it is premature to completely abandon *electroweak naturalness*² at this stage, for it is still possible to imagine models in which the bounds on superpartners are evaded in a natural manner, allowing *electroweak-natural* (at least to a large degree) models. At the same time, various mechanisms exist which can give rise to a Higgs-like particle at around 125 GeV without introducing excessive tuning. With this philosophy in mind, some approaches to (SUSY) BSM physics have generated renewed interest, such as: i) Models in which the first and second generation squarks are rather heavy, but those of the third generation are light for some reason, as in [9–15], ii) Models which have a rather special spectrum, such as a compressed one [16–18], or a stealth one [19, 20], iii) Models which do not give rise to signatures with appreciable missing energy, the prototypical example being that of baryonic R -parity violating (RPV) models (see [21] for a review), and iv) Models in which the production cross-section is small even for light first and second generation squarks, as in examples with a relatively heavy Dirac gluino [22, 23].

In [24], a model was proposed that shares some features of the RPV models and models with Dirac gluinos, mentioned above. The defining feature of this model was the existence of a $U(1)_R$ symmetry that was identified with one of the lepton numbers and the role of the sneutrino as the down-type Higgs. In [25] the R -symmetry was generalized to a global lepton number to allow for viable neutrino masses and mixings. Ref. [26] studied the case where the $U(1)_R$ symmetry is identified with the baryon number. In this paper we perform a classification of phenomenologically interesting R -symmetric models, and

¹For concreteness, we interpret the ~ 125 GeV resonance as arising from a CP-even Higgs-like particle.

²It is hard to give a precise unambiguous criterion of electroweak-naturalness, but the general notion is rather clear.

show how some of these R -symmetries are consistent with leptonic or baryonic RPV operators, and therefore provide an elegant motivation for the existence of these operators (see [27] for an alternative approach motivating RPV operators). We then focus on the case where the lepton number is tied to $U(1)_R$ symmetry, and study it in detail with the goal of laying out the LHC phenomenology.

Indeed, having an R -symmetry gives rise to many interesting phenomenological features. For example, Majorana gaugino masses, certain scalar trilinear “ A -terms”, and the “ μ -term” are forbidden. However, gaugino masses of the Dirac type are allowed.³ This leads to a significant suppression of flavor and CP-violating effects relative to the MSSM for $\mathcal{O}(1)$ flavor-violating soft scalar masses and phases [29]. Various other aspects of R -symmetric models have been studied in the literature [30–39]. Although the minimal R -symmetric spectrum does not give rise to gauge coupling unification, many scenarios for adding additional matter have been proposed which could help unify the couplings [28, 40, 41]. Particular variants of R -symmetric models can also give rise to a strong electroweak phase transition generating the observed baryon asymmetry, as well as an LSP DM candidate [42, 43]. Finally, a remarkable feature, which we will exploit in this work, is that when the R -symmetry is identified with a lepton or baryon number respectively,⁴ this allows leptonic or baryonic RPV operators in the Lagrangian consistent with these symmetries. Therefore, these are not subject to stringent constraints from lepton or baryon number violating observables, such as upper bounds on neutrino masses and nucleon-antinucleon oscillations, respectively.

R -symmetries are also well-motivated from a more theoretical point of view. In the global supersymmetric limit, it has been known for quite some time that R -symmetry plays an important role in supersymmetry breaking as it is directly related to the existence of supersymmetry breaking minima due to the Nelson-Seiberg theorem [44]. Since Majorana gaugino masses necessarily break the R -symmetry, considerable effort has been devoted to generating large-enough Majorana gaugino masses while still preserving enough R -symmetry to keep supersymmetry breaking intact. However, an alternative is to consider generic supersymmetry breaking scenarios that give rise to *Dirac* gaugino masses fully consistent with the R -symmetry.

The scope of this work is the following. We present a classification of phenomenologically viable R -symmetric models by providing a rather general description of such models in Section 2. This is done by making manifest the relevant $U(1)$ symmetries present. Then, we show that preserving different combinations of $U(1)$ symmetries gives rise to the different variants of R -symmetric models considered in the literature, including some which have been relatively poorly explored. In particular, we will see that in addition to the relatively well-studied R -symmetric models with the usual “ R -parity conserving” operators, there are models which include subsets of the so-called “ R -parity violating (RPV)” operators. However, it is important to note that while the standard R -parity is violated in these models, there is still a continuous R -symmetry and these operators are perfectly compatible with it. These kinds of R -symmetric models arise when one identifies the lepton number (L) or the baryon number (B) of the SM fermions with their R -charges, as will be clear soon. When the lepton number behaves as an R -symmetry, depending upon the region of parameter space, it is possible to

³Dirac gaugino masses can also be motivated from “supersoft” supersymmetry breaking in which the gauge sector has $\mathcal{N} = 2$ supersymmetry [28].

⁴The lepton and baryon numbers of the SM fermions are standard, but the extension of these to BSM particles is “non-standard”.

have either the usual down-type Higgs (H_d) providing masses to the down-type fermions, or have one of the sneutrinos ($\tilde{\nu}_1$) providing such masses since it also gets a vacuum-expectation value (vev). Furthermore, in the limiting case when H_d is heavy and is not part of the low-energy spectrum, then the dominant contribution to down-type masses arises from the sneutrino vev , which is *not* constrained by neutrino masses unlike that in standard RPV models. All these points will be explained in detail in the following sections. After describing the general classification of models in Section 2, in the rest of the paper we specialize to the case where the lepton number is related to the R -symmetry, as suggested by the title of the paper. We present some characteristic features of the model in Section 3, highlighting the differences from standard RPV models. The fermionic electroweak sector of the model is studied in Section 4, followed by a discussion of the existing constraints on the model from indirect effects, such as electroweak precision observables, flavor physics, etc. in Section 5. The basic aspects of the Higgs sector of these models are laid out in Section 6, in particular the region of parameter space which gives rise to a ~ 125 GeV CP-even eigenstate is explained. Finally, we describe the broad phenomenological features of the model in Section 7. Since the collider signals of these scenarios are quite interesting and novel, in this paper we discuss only the qualitative features which set them apart from other models. A more detailed treatment of collider constraints and signals is done in a companion paper [1]. Finally, we briefly discuss some aspects of Dark Matter in Section 8, followed by conclusions and future directions in Section 9. The appendices deal with some details of R -symmetry breaking operators in Appendix A, a description of a flavor ansatz for the λ and λ' couplings (the standard notation for the coefficients of the LLE^c and LQD^c operators, respectively) in Appendix B, and an estimate of the lower bound on λ'_{i33} couplings, given the observation of a lepto-quark (LQ) signal, in Appendix C.

2 Classification of R -symmetric Models

We start with the prototypical R -symmetric Standard Model studied in [29]. In addition to the superfield content of the MSSM – H_u , H_d , Q_i , U_i^c , D_i^c , L_i , E_i^c ($i = 1, 2, 3$), this includes a pair of vector-like $SU(2)_L$ doublet superfields R_u and R_d (with hypercharge $\frac{1}{2}$ and $-\frac{1}{2}$ respectively), as well as superfields in the adjoint representation of the SM gauge group: a “hypercharge adjoint” or singlet, S , an $SU(2)_L$ triplet, T (with zero hypercharge), and an $SU(3)_C$ octet, O .

The relevant global $U(1)$ symmetries of the model in [29] include an R -symmetry denoted by $U(1)_{R_0}$ along with the well known lepton number $U(1)_L$ and baryon number $U(1)_B$, as shown below in Table 1:

	Q_i	U_i^c	D_i^c	L_i	E_i^c	H_u	H_d	R_u	R_d	S	T	O
$U(1)_{R_0}$	1	1	1	1	1	0	0	2	2	0	0	0
$U(1)_L$	0	0	0	1	-1	0	0	0	0	0	0	0
$U(1)_B$	1/3	-1/3	-1/3	0	0	0	0	0	0	0	0	0

Table 1: (Super)Field content and $U(1)$ charge assignments.

The following superpotential consistent with the above symmetries was considered in [29]:

$$W_0 = y_{ij}^u H_u Q_i U_j^c + \tilde{y}_{ij}^d H_d Q_i D_j^c + \tilde{y}_{ij}^e H_d L_i E_j^c + \mu_u H_u R_d + \mu_d R_u H_d . \quad (1)$$

It is possible to also write down the following terms with adjoint superfields, consistent with all symmetries:

$$W_{adj} = S(\lambda_u^S H_u R_d + \lambda_d^S R_u H_d) + (\lambda_u^T H_u T R_d + \lambda_d^T R_u T H_d) . \quad (2)$$

It is easy to see that with the above R -charge assignments the usual ‘‘RPV’’ operators, schematically denoted by LH_u , LLE^c , LQD^c , and $U^c D^c D^c$, are forbidden. However, R -symmetries are *not* inconsistent with subsets of RPV operators in general, since it is possible to construct R -symmetries R_i ($i = 1, 2, 3$), which are linear combinations of $U(1)_{R_0}$, $U(1)_L$ and $U(1)_B$, as seen in Table 2 below:

	Q_i	U_i^c	D_i^c	L_i	E_i^c	H_u	H_d	R_u	R_d	S	T	O
$U(1)_{R_1=R_0-L}$	1	1	1	0	2	0	0	2	2	0	0	0
$U(1)_{R_2=R_0+B}$	4/3	2/3	2/3	1	1	0	0	2	2	0	0	0
$U(1)_{R_3=R_0+L}$	1	1	1	2	0	0	0	2	2	0	0	0

Table 2: (Super)Field content and three different combinations of $U(1)_R$ charge assignments.

We see that depending on the choice of the R -symmetry, the following RPV operators are allowed in the superpotential, *in addition* to those in (1) and (2):

$$\begin{aligned} W_1 &= W_0 + W_{adj} + \lambda_{ijk} L_i L_j E_k^c + \lambda'_{ijk} L_i Q_j D_k^c , & (R_1 = R_0 - L) \\ W_2 &= W_0 + W_{adj} + \lambda''_{ijk} U_i^c D_j^c D_k^c , & (R_2 = R_0 + B) \\ W_3 &= W_0 + W_{adj} + \mu_L^{(i)} H_u L_i . & (R_3 = R_0 + L) \end{aligned} \quad (3)$$

In principle, the term $\mu_L^{(i)} R_u L_i$ is also allowed for $R = R_1$, but it is possible to do an $SU(4)$ field redefinition of the L_i and H_d , and define ‘‘ H_d ’’ as the field which couples to R_u , leading to (3).

Thus, this provides a rather general classification of phenomenologically viable R -symmetric Standard Models. The choice $R = R_1$ corresponds to identifying the lepton numbers of the SM fermions with (the negative of) their R -charges, while the choice $R = R_3$ corresponds to identifying them with their R -charges. The choice $R = R_2$ on the other hand identifies the baryon numbers of the SM fermions with their R -charges, and has been considered in [26]. Note that since the R -symmetries $R_{1,2,3}$ are identified with lepton or baryon number, they are anomalous and should therefore be thought of as accidental low-energy symmetries just like the latter (note that R_0 is non-anomalous). The above are special limits of a generic $U(1)_{\hat{R}}$ symmetry with $\hat{R} = R + aL + bB$ for real a and b . However, all other cases are severely constrained by proton decay bounds, and we do not consider them any further.

As we will see later, even though the R -symmetries R_1, R_2 and R_3 allow RPV operators, they are less constrained than standard RPV models with the same operators. The basic reason for this is that in these models these RPV operators are consistent with lepton or baryon numbers (which

are identified with the R -symmetries above), hence there are no constraints on the couplings of these operators from processes which violate lepton or baryon number.

2.1 Supersymmetry Breaking

In order to fully specify the lagrangian, supersymmetry breaking terms must be included. Since we are interested in R -symmetric models, we imagine a situation in which supersymmetry breaking (at least in the global limit) is *not* accompanied by R -breaking. This can happen if supersymmetry breaking is of the D -type, as described in [45]. This includes both D -term SUSY breaking parametrized by a spurion superfield $\mathcal{W}'_\alpha = \lambda'_\alpha + \theta_\alpha D'$ with $R[\mathcal{W}'_\alpha] = 1$ ($R[\lambda'_\alpha] = 1, R[D'] = 0$) and $\langle D' \rangle \neq 0$, as well as F -term supersymmetry breaking parametrized by a spurion superfield $X = x + \theta^2 F_X$ with $R[X] = 2$ and $\langle x \rangle = 0, \langle F_X \rangle \neq 0$.

We follow the same procedure as before, by first considering soft terms consistent with the original R -charge assignments ($R = R_0$) as in Table 1, and then studying additional terms allowed by the other choices - $\{R_1, R_2, R_3\}$ in Table 2.

The spurion \mathcal{W}'_α generates “supersoft” terms via⁵

$$\sqrt{2} \int d^2\theta \frac{\mathcal{W}'_\alpha}{M_\star} [c_1 \mathcal{W}'_\alpha S + c_2 \mathcal{W}'_\alpha T^i + c_3 \mathcal{W}'_\alpha O^a] + \text{h.c.} , \quad (4)$$

which contain Dirac gaugino masses $m_{D_i} = c_i D' / M_\star$. Here M_\star denotes the scale of SUSY breaking mediation (e.g. the messenger scale in Dirac gauge-mediation scenarios). The above terms preserve a $U(1)_R$ symmetry under which the \mathcal{W}'_α and \mathcal{W}'_α have R -charge⁶ 1, while $R[S] = R[T^i] = R[O^a] = 0$.

The spurion X generates the following $U(1)_R$ -preserving renormalizable soft terms:

$$L_0^{\text{soft}} = \sum_i m_i^2 \Phi_i^\dagger \Phi_i + \left[t_S S + \frac{1}{2} b_S S^2 + \frac{1}{3} A_S S^3 + \frac{1}{2} b_T T^2 + \frac{1}{2} b_O O^2 + B\mu H_u H_d \right. \\ \left. + A_S S H_u H_d + A_T H_u T H_d + A_T^\lambda S T^2 + A_O^\lambda S O^2 + \text{h.c.} \right] , \quad (5)$$

where the sum runs over all the scalars, and we denote the scalar components by the same notation used for the superfields. These are generated via the following operators:

$$\int d^4\theta \frac{X^\dagger X}{M_\star^2} \left\{ \sum_i \Phi_i^\dagger \Phi_i + \left[H_u H_d + \epsilon M_\star S + S^2 + T^2 + O^2 + \frac{1}{M_\star} \times \text{cubic} + \text{h.c.} \right] \right\} , \quad (6)$$

$$\int d^2\theta \frac{X}{M_\star} (S T^2 + S O^2 + S^3) + \text{h.c.} . \quad (7)$$

We can see that operators quadratic in the visible superfields in the first line in (6) are of order $\frac{|F_X|^2}{M_\star^2}$.

⁵The \mathcal{W}'_α are the $SU(3)_C \times SU(2)_L \times U(1)_Y$ chiral superfield strengths.

⁶The choice $R[\mathcal{W}'_\alpha] = R[\mathcal{W}'_\alpha] = 1$ is dictated by the SUSY gauge kinetic terms; in particular this always implies $R[\lambda_\alpha] = R[\lambda'_\alpha] = 1$.

We take $F_X \sim D'$ and

$$\frac{F_X}{M_\star} \equiv M_{\text{SUSY}} \sim 100 \text{ GeV} - 1 \text{ TeV} . \quad (8)$$

So Dirac gaugino masses from (4), and the non-holomorphic soft mass-squareds, and B -terms from (6) are parametrically of the same order (although there may be modest numerical hierarchies). The operators which are cubic and higher order in the visible superfields in Eq. (6) will be suppressed by powers of M_{SUSY}/M_\star , and are therefore very suppressed. For the linear term in S in (5), dimensional analysis generically gives a coefficient t_S of order $M_\star M_{\text{SUSY}}^2$. Phenomenologically however, t_S should not be larger than M_{SUSY}^3 , since otherwise the scalar singlet tadpole, $t_S S$, will destabilize the hierarchy. Ref. [46] has recently argued that this is indeed the case in these scenarios, so that one has $\epsilon \ll 1$.

The operators in the second line in (7) can give trilinear A -terms involving the adjoint fields of order $\frac{|F_X|}{M_\star} \sim M_{\text{SUSY}}$ if allowed. However, these are forbidden if X is not a gauge singlet, implying that the scale of these operators can be easily suppressed relative to those in the first line, whose scale is naturally set by M_{SUSY} . Finally, note that since we imagine that X belongs to a hidden sector which has no direct couplings to the observable sector superfields above, there are no terms like $\int d^2\theta X[M_\star S + H_u H_d + S^2 + T^2 + O^2]$ (due to the non-renormalization theorem, it is technically natural to omit these superpotential couplings).

With other choices for the R -symmetry - R_1 , R_2 and R_3 , as described in Table 2, one can write down additional soft supersymmetry breaking operators as follows:

$$\begin{aligned} L_1^{\text{soft}} &= L_0^{\text{soft}} + B\mu_L^{(i)} H_u L_i + A_S^{(i)} S H_u L_i + A_T^{(i)} H_u T L_i , & R_1 &= R_0 - L \\ L_2^{\text{soft}} &= L_0^{\text{soft}} , & R_2 &= R_0 + B \\ L_3^{\text{soft}} &= L_0^{\text{soft}} . & R_3 &= R_0 + L \end{aligned} \quad (9)$$

Only the case $R_1 = R_0 - L$ allows additional gauge-invariant operators consistent with the R -symmetry (since L has zero R -charge). These additional soft terms for the case $R = R_1$ in (9) give rise to a very interesting possibility for the vacuum structure of the theory.

The presence of the $B\mu_L^{(i)}$ term in (9) for $R = R_1$ implies that one of the left-handed sneutrinos gets a vev ⁷ due to a tadpole for the sneutrino when H_u gets a vev . It then becomes possible to distinguish two extreme cases: i) $\langle \tilde{\nu}_1 \rangle \ll \langle H_d^0 \rangle$, and ii) $\langle \tilde{\nu}_1 \rangle \gg \langle H_d^0 \rangle$. In fact the size of the $\mu_d R_u H_d$ term in superpotential W_0 controls which one is relevant. This is because, schematically,

$$\langle \tilde{\nu}_1 \rangle \sim \frac{B\mu_L^{(1)}}{m_{\tilde{L}}^2} v_u , \quad \langle H_d^0 \rangle \sim \frac{B\mu}{\mu_d^2} v_u \quad \implies \quad \frac{\langle H_d^0 \rangle}{\langle \tilde{\nu}_1 \rangle} \sim \frac{B\mu}{B\mu_L^{(1)}} \frac{m_{\tilde{L}}^2}{\mu_d^2} . \quad (10)$$

Here $m_{\tilde{L}}$ is the soft mass of the left-handed sleptons. Thus, if $\mu_d^2 \gg m_{\tilde{L}}^2$, then $\langle \tilde{\nu}_1 \rangle \gg \langle H_d^0 \rangle$.

⁷Recall that we have defined “ H_d ” as the linear combination of $SU(2)_L$ doublets with $Y = -1/2$ and $R = 0$, that couples to R_u in the superpotential. Within this class of bases, it is further possible, by $SU(3)$ rotations, to go to the “single- vev -basis” where only one of the three L_i acquires a vev (see Section 3). We will see later that the most natural choice is to identify the direction of this vev with the “electron” direction, i.e. $i = 1$. The H_d vev in this basis may be non-vanishing, but we are interested in a region of parameter space where it is small compared to the EW scale.

In the remainder of this paper, we will study the choice $R = R_1$ and the case $\langle \tilde{\nu}_1 \rangle \gg \langle H_d^0 \rangle$ in detail as it gives rise to rather novel and interesting phenomenology. We will discuss the phenomenology of the $R = R_2$ case in Section 7.6 very briefly, since that case has already been considered in [26]. For the case we are interested in, the superpotential in (1), (2) and the soft terms in (5), (9) can be simplified since the large μ_d term allows us to integrate out the fields R_u and H_d , leading to the following:

$$W = \mu_u H_u R_d + \lambda_u^S S H_u R_d + \lambda_u^T H_u T R_d + y_{ij}^u H_u Q_i U_j^c + \lambda_{ijk} L_i L_j E_k^c + \lambda'_{ijk} L_i Q_j D_k^c, \quad (11)$$

$$L_{soft} = \sum_i m_i^2 \Phi_i^\dagger \Phi_i + \left[t_S S + \frac{1}{2} b_S S^2 + \frac{1}{2} b_T T^2 + \frac{1}{2} b_O O^2 + B \mu_L^{(i)} H_u L_i + \frac{1}{3} A_S S^3 + A_T^\lambda S T^2 + A_O^\lambda S O^2 + A_S^{(i)} S H_u L_i + A_T^{(i)} H_u T L_i + \text{h.c.} \right], \quad (12)$$

where the terms in the second line in L_{soft} are assumed to be suppressed relative to M_{SUSY} for simplicity, from the arguments below (7). *Note that in the $R = R_1$ scenario the down-type masses arise from the LLE^c and LQD^c operators when the left-handed sneutrino gets a vev (assuming $\langle H_d^0 \rangle \ll \langle \tilde{\nu}_1 \rangle$).*

2.2 R -breaking

It is well-known that the vanishingly small value of the cosmological constant breaks R -symmetry since it requires a non-zero value of the superpotential in the vacuum, and the superpotential has non-zero R -charge. Since the gravitino mass $m_{3/2} \sim \langle W \rangle$ (in Planck units), this implies that $m_{3/2}$ is the order parameter of R -breaking. As mentioned in the Introduction, in this work we imagine a setup in which $m_{3/2}$ is much smaller than the TeV scale. Hence, the effects of R -breaking are also small.

The breaking of R -symmetry will eventually be transmitted to the visible sector. This can essentially happen in two ways. A simple possibility is that R -breaking is mediated to the visible sector by generic Planck suppressed operators, which we denote as “generic gravity mediation”. This is a natural possibility since gravity is expected to violate all global symmetries in general. However, another possibility is that these generic Planck suppressed operators respect the R -symmetry (at least to a very good approximation) due to it being an accidental symmetry of the visible sector, see [47] for an example. In this case R breaking will generically be communicated to the visible sector via anomaly mediation.

In fact, the source of R -breaking can be connected to observable physics in an interesting way. For example, for $R = R_1$ the breaking of the R -symmetry will give rise to neutrino masses [24, 25], while for $R = R_2$, R -breaking will give rise to nucleon-antinucleon oscillations and may also lead to proton decay in certain cases [26]. Existing constraints from these observables then put an upper bound on $m_{3/2}$ and therefore on the messenger scale, M_* , as well [24]. In Appendix 2.2, we describe some details of the sizes of R -breaking operators. However, the collider phenomenology is largely determined by the approximate R -symmetry, and therefore we will often focus on the R -symmetric limit. A more thorough analysis of the full effects of R -breaking is left for the future.

3 Characteristic Features of the Model with $R = R_1$

In the R -symmetric limit, the superpotential and soft terms are given by Eqs. (11) and (12). The terms including the lepton (super) fields above are written in a general basis. In a general basis, all the sneutrino fields can develop non-vanishing vacuum expectation values (vev 's) since there are $B\mu_L$ terms for all of them. However, it is always possible to choose a basis in which only one of the sneutrino fields gets a vev [25].⁸ In this sense, there is a similarity with models of R -parity violation (RPV) where the H_d and L_i fields mix, in general, with each other, giving rise to mass eigenstates $L_\alpha, \alpha = 1, \dots, 4$. There is an important difference, however, since H_d has been integrated out, and the “light down-type doublet”, R_d , has a different R -charge from the L_i . Thus, there is only a three-dimensional space in which the (sneutrino) fields can mix. We will follow the analysis in [21] keeping this difference in mind.

The general basis can be related to the “single vev basis” as:

$$L_i = \frac{v_i}{v_{(a)}} L_{(a)} + \sum_b e_{ib} L_b . \quad (13)$$

Here the lepton of flavor (a) is assumed to get a vev , while i, j, k run over all three generations and b (and later c) runs over only two generations (those which do not get a vev). The e_{ib} are the matrix elements that relate the fields in the two bases. There is still the freedom to rotate L_b , and by choosing an appropriate e_{ib} one can go to a basis in which the charged Yukawa couplings are diagonal.

Since the lepton Yukawa coupling is provided by the $\lambda_{ijk} L_i L_j E_k^c$ operator, and λ_{ijk} is antisymmetric in the first two indices, gauge invariance prevents the lepton of flavor (a) from getting a mass from such operators. Its mass can, nevertheless, be generated from supersymmetry breaking (but R -preserving) operators. For example, it could come from the following operators:

$$\begin{aligned} i) \quad & y'_{(1)} \int d^4\theta \frac{X^\dagger}{M_\star^2} H_u^\dagger L_{(a)} E_{(a)}^c , & ii) \quad & y'_{(2)} \int d^4\theta \frac{X^\dagger X}{M_\star^2} H_u^\dagger \frac{\mathcal{D}_\alpha L_{(a)} \mathcal{D}_\alpha E_{(a)}^c}{4\mu_d^2} , \\ \Delta m_L^{(1)} = & y'_{(1)} \frac{|F_X|}{M_\star^2} v_u \sim \left(\frac{M_{\text{SUSY}}}{M_\star} \right) v_u , & \Delta m_L^{(2)} = & y'_{(2)} \frac{|F_X|^2}{M_\star^2} \frac{v_u}{4\mu_d^2} \sim \left(\frac{M_{\text{SUSY}}^2}{4\mu_d^2} \right) v_u . \end{aligned} \quad (14)$$

We see that the first operator can provide viable lepton masses only if the messenger scale M_\star is low [24, 48], but the second operator is generated after integrating out the fields R_u and H_d with a large supersymmetric mass term $\mu_d R_u H_d$ (see discussion around (10), and appendix B in [42]), and can give a viable contribution even if the messenger scale M_\star is high. Note that both these operators are present for all lepton flavors in general, so these will provide contributions to lepton masses *in addition* to those from the superpotential in (11).⁹ Therefore, the smallness of the electron mass makes it natural to take (a) = 1 (e), and $b, c = 2$ (μ), 3 (τ), so that the electron gets its mass *solely* from supersymmetry breaking (but R -preserving) operators in (14) [25]. We will assume this henceforth.

⁸The physics is of course basis independent.

⁹They will also contain flavor off-diagonal entries, presumably of order m_e . In the lepton mass eigenbasis, these will induce off-diagonal slepton masses, even if these are diagonal (but not degenerate) in the gauge eigenbasis. In this R -symmetric framework, we expect the constraints from $\mu \rightarrow e\gamma$ and $\mu - e$ conversion in nuclei to be satisfied since the mixing angles are of order m_e/m_μ and because we take the Dirac bino mass M_1^D around 1 TeV (see section 7) [49].

In the “single-vev” and “mass-eigenstate” basis, the superpotential is given by:

$$\begin{aligned}
W &= \mu_u H_u R_d + \lambda_u^S S H_u R_d + \lambda_u^T H_u T R_d + W_{\text{Yukawa}} + W_{\text{Trilinear}} , \\
W_{\text{Yukawa}} &= \sum_{b=2,3} y_b^{(e)} \hat{L}_{(a)} \hat{L}_b \hat{E}_b^c + \sum_{i=1,2,3} y_i^{(d)} \hat{L}_{(a)} \hat{Q}_i \hat{D}_i^c , \\
W_{\text{Trilinear}} &= \sum_{i=1,2,3} \lambda_{23i} \hat{L}_2 \hat{L}_3 \hat{E}_i^c + \sum_{i,j=1,2,3;b=2,3} \lambda'_{bij} \hat{L}_b \hat{Q}_i \hat{D}_j^c .
\end{aligned} \tag{15}$$

where the hat denotes that the lepton and quark fields are in the “mass-eigenstate” basis. Note that the first two indices in the trilinear term LLE^c in $W_{\text{Trilinear}}$ in Eq. (15) are fixed to be (2) and (3) since $(a) = (1)$, and since the coupling is antisymmetric in the first two indices. There is, however, no such antisymmetry for the first two indices in the LQD^c term in $W_{\text{Trilinear}}$. Overall, these terms have a rather different flavor structure compared to analogous trilinear RPV couplings in RPV models [21].

To contrast some other important features of our model against RPV models considered in the literature, it is instructive to look at properties of standard RPV models with both bilinear and trilinear RPV operators, where we use the established results summarized in [21]. For example, the presence of the fermionic and scalar bilinear RPV operators in such models is associated with mixing between neutrinos and neutralinos (or charged leptons and charginos). In particular, the superpotential bilinear $\mu'_i \tilde{H}_u L_i$ generates neutrino masses at tree-level proportional to $\tan^2 \xi$ through such mixings, where the angle ξ parametrizes the physical higgsino-lepton mixing in the fermion sector (which cannot be rotated away) in a basis-independent way. This leads to a very stringent bound, $\sin \xi \lesssim 3 \times 10^{-6} \sqrt{1 + \tan^2 \beta}$. Hence, in the basis with a single μ -term (i.e. $\hat{\mu} H_u H_d$, but no $\mu'_i H_u L_i$), the sneutrino *vevs* are forced to be extremely small due to the upper bound on neutrino masses. Furthermore, the presence of the scalar bilinear RPV operator $B\mu_L^{(i)} H_u L_i$ in $\mathcal{L}_{\text{soft}}$ and the trilinear RPV operators λLLE^c , $\lambda' LQD^c$ in the superpotential, give rise to one-loop contributions to neutrino masses proportional to i) $g^2 (B\mu_L^{(i)})^2$, ii) $g\lambda'$ (or $g\lambda$), iii) λ'^2 or (λ^2) ,¹⁰ which put stringent bounds on many λ, λ' couplings (such as λ_{i33} and λ'_{i33} , $i = 1, 2, 3$) as well as the size of $B\mu_L^{(i)}$ (this can also be interpreted as putting a stringent bound on the sneutrino *vev*'s through the basis-independent Higgs-slepton mixing angle $\sin \zeta$, even in the absence of the superpotential bilinear RPV operator).

In the model under consideration, the operators λLLE^c and $\lambda' LQD^c$ in the superpotential, and the operator $B\mu_L^{(i)} H_u L_i$ in $\mathcal{L}_{\text{soft}}$, preserve a lepton number (which is identified with the R -symmetry $R = R_1$), unlike that in standard RPV models above. Hence these terms cannot generate Majorana neutrino masses which violate the lepton number ($R = R_1$) either at tree-level or loop-level, as long as the R -symmetry is conserved. This further implies that the sneutrino *vev* (induced by the $B\mu_L^{(i)}$ term) can be significant and can play the role of a Higgs field. Also note that there is no $\mu'_i \tilde{H}_u L_i$ term in the Lagrangian, implying that the basis in which the Yukawa couplings in W_{Yukawa} are diagonal is the same as the mass-eigenstate basis of the charged leptons, unlike in RPV models [21].

Finally, from above we see that the bounds on neutrino masses are only relevant when R -breaking effects are taken into account and are, hence, proportional to $m_{3/2}$ (see Section 2.2). Thus, for given values of the sneutrino *vev* and the λ, λ' couplings (which are consistent with other constraints, see

¹⁰Here g schematically denotes any of the two electroweak gauge couplings.

Section 5), the bounds from neutrino masses only provide a bound on $m_{3/2}$.

4 The Fermionic Electroweak Sector

Since in our framework lepton number is identified with an R -symmetry ($R = R_1$), the neutralinos and neutrinos on the one hand, and charginos and charged leptons on the other, share the same quantum numbers (in particular, their R -charge). They can, therefore, mix after electroweak symmetry breaking.

4.1 Charginos & Charged Leptons

The charginos and charged leptons will mix after electroweak symmetry breaking in general. However, from (15), it is clear that only the charged lepton of flavor (a) (the electron since $(a) = 1$) will mix with the charginos since only that flavor gets a vev . One has four *Dirac* charginos (one of which is the electron), which can be further split according to their electric and R -charges. Then, one can form two groups of 2-component fields - one with $R = +Q$, and one with $R = -Q$. This implies that the chargino mass matrix can be written as:

$$\begin{aligned} \mathcal{L}_C &= ((\tilde{\chi}^{++})^T (\tilde{\chi}^{+-})^T) \begin{pmatrix} \mathbf{M}_C^{(+)} & 0 \\ 0 & \mathbf{M}_C^{(-)} \end{pmatrix} \begin{pmatrix} \tilde{\chi}^{--} \\ \tilde{\chi}^{-+} \end{pmatrix}, \\ \tilde{\chi}^{++} &= (\tilde{w}^+, e_R^c), \quad \tilde{\chi}^{--} = (\tilde{T}_d^-, e_L^-), \quad (\text{for } R = +Q) \\ \tilde{\chi}^{-+} &= (\tilde{w}^- \tilde{R}_d^-), \quad \tilde{\chi}^{+-} = (\tilde{T}_u^+, \tilde{H}_u^+), \quad (\text{for } R = -Q) \end{aligned} \quad (16)$$

where

$$\mathbf{M}_C^{(+)} = \begin{pmatrix} M_2^D & gv_{(a)} \\ 0 & m_e \end{pmatrix}, \quad \mathbf{M}_C^{(-)} = \begin{pmatrix} M_2^D & \sqrt{2}\lambda_u^T v_u \\ gv_u & -\mu_u - \lambda_u^S v_s + \lambda_u^T v_T \end{pmatrix}. \quad (17)$$

The notation $\tilde{\chi}^{+-}$, for instance, implies that the field $\tilde{\chi}$ has electric charge +1 and R -charge -1. Here M_2^D stands for the Dirac wino mass, g is the $SU(2)$ gauge coupling, m_e is the electron mass, and v_u , $v_{(a)}$, v_s & v_T are the vev 's of H_u^0 , $\tilde{\nu}_{(a)}$, S and T^0 respectively. The above matrices can be diagonalized by two pairs of 2×2 matrices - $\{\mathbf{V}^+, \mathbf{U}^+\}$ for $(\tilde{\chi}^{++} \tilde{\chi}^{--})$, and $\{\mathbf{V}^-, \mathbf{U}^-\}$ for $(\tilde{\chi}^{+-} \tilde{\chi}^{-+})$, respectively, such that $(\mathbf{V}^+)^\dagger \mathbf{M}_C^{(+)} \mathbf{U}^+$ and $(\mathbf{V}^-)^\dagger \mathbf{M}_C^{(-)} \mathbf{U}^-$ are diagonal (and with positive eigenvalues). The above states are naturally arranged into four 4-component Dirac fields $\tilde{X}_i^{++} = (\tilde{\chi}_i^{++} \tilde{\chi}_i^{--})$ and $\tilde{X}_i^{+-} = (\tilde{\chi}_i^{+-} \tilde{\chi}_i^{-+})$, with $i = 1, 2$, whose charge conjugates are denoted by \tilde{X}_1^{--} and \tilde{X}_i^{-+} respectively. In this notation, $e \equiv \tilde{X}_1^{--}$ corresponds to the physical (Dirac) electron field.

4.2 Neutralinos & Neutrinos

Similar to the charged fermion sector, the neutralinos and neutrinos in the neutral fermion sector will mix after electroweak symmetry breaking. For simplicity, we consider only one neutrino generation since adding the other neutrinos does not change the qualitative collider picture (see [25] for a thorough

discussion of neutrino masses and mixings). Also, since Majorana neutrino masses violate lepton number (hence R symmetry in our case), they are massless in the R -symmetric limit.¹¹ It is convenient to write the matrix in the ‘‘Dirac’’ basis by grouping the fields with R -charges $+1$ and -1 separately.

Then, similar to the charginos, the mass terms for the neutralinos can be written as $\mathcal{L}_N = (\tilde{\chi}^{0+})^T \mathbf{M}_N \tilde{\chi}^{0-}$ where $\tilde{\chi}^{0+} = (\tilde{b}^0, \tilde{w}^0, \tilde{R}_d^0)$ and $\tilde{\chi}^{0-} = (\tilde{S}, \tilde{T}^0, \tilde{H}_u^0, \nu_e)$. The notation $\tilde{\chi}^{0+}$ implies that the field $\tilde{\chi}$ has vanishing electric charge and R -charge $+1$. The mass matrix M_N is given by:

$$\mathbf{M}_N = \begin{pmatrix} M_1^D & 0 & \frac{g' v_u}{\sqrt{2}} & -\frac{g' v_{(a)}}{\sqrt{2}} \\ 0 & M_2^D & -\frac{g v_u}{\sqrt{2}} & \frac{g v_{(a)}}{\sqrt{2}} \\ \lambda_u^S v_u & \lambda_u^T v_u & \mu_u + \lambda_u^S v_s + \lambda_u^T v_T & 0 \end{pmatrix}. \quad (18)$$

After diagonalizing the above mass matrix by unitary transformations \mathbf{V}^N and \mathbf{U}^N , as in the chargino case above, one obtains three *Dirac* mass eigenstates $\tilde{X}_i^{0+} \equiv (\tilde{\chi}_i^{0+}, \tilde{\chi}_i^{0-})$, with $i = 1, 2, 3$, and one massless *Weyl* neutralino $\tilde{\chi}_4^{0-}$ that necessarily remains massless, which is identified with the massless neutrino eigenstate, and is given in general by:

$$\tilde{\chi}_4^{0-} = U_{4\tilde{s}}^N \tilde{S} + U_{4\tilde{t}}^N \tilde{T}^0 + U_{4u}^N \tilde{H}_u^0 + U_{4\nu}^N \nu_e. \quad (19)$$

By a slight abuse of notation, sometimes we will also refer to $\tilde{\chi}_4^{0-}$ as ‘‘ ν_e ’’, where it will always refer to the mass eigenstate, and should not be confused with the original gauge eigenstate.

5 Indirect Constraints

The identification of the lepton numbers of SM fermions with (the negative of) their R -charges is subject to various ‘‘indirect’’ constraints. As explained in Section 3, the sneutrino vev can be significant in these models since there are no bounds from neutrino masses. Thus, the most stringent constraints in these models arise from electroweak precision measurements and from flavor violating processes [24,25]. We will see that these can be satisfied in a large range of parameter space and for reasonable flavor-off diagonal couplings. Many of the constraints are similar to those studied in [24]. It is convenient to divide the constraints into two categories:

- Constraints on the sneutrino vev $v_{(a)}$, or equivalently $\tan \beta \equiv \frac{v_u}{v_{(a)}}$.
- Constraints on the λ and λ' couplings.

5.1 Constraints on the sneutrino vev $v_{(a)}$ ($\tan \beta$)

First, the mixing between the charged leptons and charginos gives rise to a deviation in the couplings of the Z to charged leptons in general, which is constrained by electroweak precision measurements. As shown in the previous section, since only one lepton (of flavor (a)=1) mixes with the charginos, the

¹¹We are assuming that there are no right-handed neutrinos with R -charges such as to allow writing down Dirac neutrino mass terms consistent with the R -symmetry.

mixing is identical to that in [24], giving rise to the following deviation in the vector and axial-vector coupling to the Z from those in the SM:

$$\begin{aligned} \delta g_V^i &= \delta g_A^i = -\frac{\sin^2 \phi}{2}, \\ \sin \phi &= -\frac{\left(m_e^2 + g^2 v_{(a)}^2 - (M_2^D)^2\right) + \sqrt{\left[m_e^2 + g^2 v_{(a)}^2 + (M_2^D)^2\right]^2 - 4 m_e^2 (M_2^D)^2}}{2 g v_{(a)} M_2^D}. \end{aligned} \quad (20)$$

From the measured value of the coupling $g_A^e = -0.50111 \pm 0.00035$ [50], one gets an upper bound on $\left(\frac{v_{(a)}}{M_2^D}\right)$. For example, for $M_2^D = 1500$ GeV (300 GeV), the current data puts an upper bound $v_{(a)} \lesssim 61$ GeV (12 GeV) at 1σ . In this work, we assume that the (Dirac) gauginos are heavier than the scalars. As a benchmark, we take $M_2^D \simeq 1.5$ TeV henceforth, implying that $v_{(a)}^{max} \simeq 60$ GeV. The fact that only the charged lepton of flavor (a) (e in our case) mixes with the charginos also gives rise to constraints from charged current universality. However, the bounds from these are not as strong as those derived from the Z -coupling above (see [24]). A lower bound on $v_{(a)}$, however, arises from leptonic Yukawa couplings, y_τ in particular. This is because the leptonic Yukawa couplings arise from the LLE^c operator, and hence are part of the λ couplings [see Eq. (11)]. Therefore, these give rise to extra tree-level contributions to electroweak observables similar to those in traditional RPV models (for a review of constraints in RPV models, see [21]). One finds that the dominant constraint arises from the τ Yukawa coupling ($y_\tau \equiv y_3^{(e)} \equiv \lambda_{133}$) contributing to the ratio $R_\tau \equiv \Gamma(\tau \rightarrow e \bar{\nu}_e \nu_\tau) / \Gamma(\tau \rightarrow \mu \bar{\nu}_\mu \nu_\tau)$ [24], as shown in Fig. 1 (R_τ is normalized to the dominant τ decay due to W exchange). This gives:

$$y_\tau < 0.07 \left(\frac{m_{\tilde{\tau}_R}}{100 \text{ GeV}} \right), \quad (21)$$

which puts a lower bound $v_{(a)} \gtrsim 8$ GeV (2.5 GeV) for $m_{\tilde{\tau}_R} = 300$ GeV (1 TeV). Since in our framework, one of the sneutrinos behaves as a Higgs field which is expected to be around the electroweak scale, it is natural to expect that the masses of all sleptons are around the electroweak scale, i.e. few hundred GeV (see more discussion on this in Section 7). We, therefore, take $v_{(a)}^{min} \simeq 10$ GeV. Combining with the upper bound on $v_{(a)}$ from above, we obtain the range:

$$\begin{aligned} 10 \text{ GeV} &\lesssim v_{(a)} \lesssim 60 \text{ GeV}, \\ \text{or} \quad 17.4 &\gtrsim \tan \beta \gtrsim 2.7, \end{aligned} \quad (22)$$

where $\tan \beta = v_u / v_{(a)}$, which we use in our subsequent analysis. Thus, we see that the sneutrino vev can be much larger than in standard (bilinear) RPV models. This is one of the most distinctive features of the model, and it also plays a crucial role in LHC phenomenology as we will see. In Section 7, we

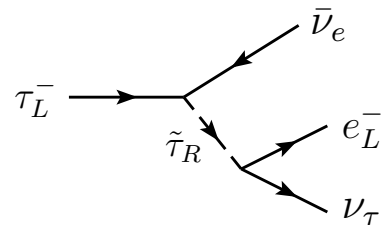


Figure 1: Contribution to the decay width $\tau_L^- \rightarrow e_L^- \bar{\nu}_e \nu_\tau$, where both the interaction vertices correspond to the τ Yukawa coupling $y_\tau \equiv \lambda_{133}$. The arrows indicate R -number flow.

will discuss how the existence of such a large sneutrino vev could be inferred at the LHC.

5.2 Constraints on λ and λ' couplings

As explained at the end of Section 3, in our model the bounds from neutrino masses can be interpreted as a bound on the gravitino mass (since it is the order parameter of R -breaking), implying that the bounds on λ, λ' couplings only arise from other observables, such as flavor-violating processes. We will see that this has an important effect on the bounds on the λ_{i33} and λ'_{i33} ($i = 1, 2, 3$) couplings in particular, because in standard RPV models the most stringent bounds ($\lambda_{i33}, \lambda'_{i33} \lesssim 10^{-3}$) on these arise from neutrino masses.¹² On the other hand, the upper bounds on λ_{i33} and λ'_{i33} in our model arise from flavor-violating processes and can be rather mild as we will see.

Constraints from flavor-violating processes in the lepton and hadron sector provide bounds on the λ and λ' couplings. Although there do exist bounds on single couplings, they are typically weak, and most of the stringent bounds arise from the products of two couplings. These can be classified into three categories, those constraining i) $\lambda\lambda$ couplings, ii) $\lambda\lambda'$ couplings, and iii) $\lambda'\lambda'$ couplings. We take our results from the general analysis of constraints arising from RPV operators in [21, 51–53]. However, as mentioned above, in our framework the lepton and down-type Yukawa couplings are part of the λ and λ' couplings respectively, and the results of [21, 51–53] must be interpreted accordingly. In particular, using the notation in (15), $\lambda_{122} \equiv y_2^{(e)}$ and $\lambda_{133} \equiv y_3^{(e)}$, while $\lambda'_{111} \equiv y_1^{(d)}$, $\lambda'_{122} \equiv y_2^{(d)}$, and $\lambda'_{133} \equiv y_3^{(d)}$. The remaining λ, λ' couplings are included in $W_{\text{Trilinear}}$ in (15). Among these non-Yukawa trilinear couplings, there are only three independent couplings of the λ -type¹³ – λ_{23i} ($i = 1, 2, 3$), and two 3×3 matrices of the λ' -type – λ'_{2jk} and λ'_{3jk} with independent entries. Thus, not only the number of independent couplings is greatly reduced, but also the implications of these bounds on the parameter space of the model are very different compared to those within a standard RPV scenario.

Coupling(s)	Upper Bound	Process
$ \lambda_{23k} ; k=1,2,3$	$0.07 \tilde{e}_{kR}$	$[R_\tau, R_{\tau\mu}]$ [21, 51]
$ \lambda_{231} y_3^{(e)} $ or, $ \lambda_{231} $	$5.2 \times 10^{-4} [\tilde{\nu}_{L_2}]^2$ $0.052 \cos \beta [\tilde{\nu}_{L_2}]^2$	$[\tau \rightarrow ee\bar{\mu}]$ [52]
$ \lambda_{232} y_3^{(e)} $ or, $ \lambda_{232} $	$7.0 \times 10^{-4} [\tilde{\nu}_{L_2}]^2$ $0.070 \cos \beta [\tilde{\nu}_{L_2}]^2$	$[\tau \rightarrow \mu e\bar{\mu}]$ [52]
$ \lambda_{233} y_3^{(e)} $ or, $ \lambda_{233} $	2.2×10^{-4} $0.022 \cos \beta$	$[\tau \rightarrow eP^0/\mu - e \text{ in nuclei}]$ [53]

Table 3: Some upper bounds on λ couplings from various flavor-violating processes. Here $[\tilde{\nu}_{L_2}]^2 \equiv (\frac{m_{\tilde{\nu}_{L_2}}}{100 \text{ GeV}})^2$. The notation for the processes is the same as in the corresponding references.

¹²In standard RPV models, the contributions from λ, λ' couplings are proportional to the quark and lepton masses, hence the bounds are rather tight for the third generation (s)quarks: λ_{i33} and λ'_{i33} , for $i = 1, 2, 3$.

¹³Note that the first two indices in the λ couplings are anti-symmetric.

Coupling(s)	Upper Bound(s)	Process
$ \lambda'_{211} y_2^{(e)} $ or, $ \lambda'_{211} $	$2.1 \times 10^{-8} [\tilde{\nu}_{L_2}]^2$ $3.5 \times 10^{-5} \cos \beta [\tilde{\nu}_{L_2}]^2$	$[\mu - e \text{ in nuclei}]$ [21, 51]
$ \lambda'_{212} y_2^{(e)} $ or, $ \lambda'_{212} $	$6.0 \times 10^{-9} [\tilde{\nu}_{L_2}]^2$ $1.01 \times 10^{-5} \cos \beta [\tilde{\nu}_{L_2}]^2$	$[K_L^0 \rightarrow \mu \bar{e}/e \bar{\mu}]$ [52]
$ \lambda'_{213} y_2^{(e)} $ or, $ \lambda'_{213} $	$1.3 \times 10^{-5} [\tilde{\nu}_{L_2}]^2$ $0.022 \cos \beta [\tilde{\nu}_{L_2}]^2$	$[B_d^0 \rightarrow e \bar{\mu}]$ [52]
$ \lambda'_{221} y_2^{(e)} $ or, $ \lambda'_{221} $	$6. \times 10^{-9} [\tilde{\nu}_{L_2}]^2$ $1.01 \times 10^{-5} \cos \beta [\tilde{\nu}_{L_2}]^2$	$[K_L^0 \rightarrow \mu \bar{e}/e \bar{\mu}]$ [52]
$ \lambda'_{222} y_2^{(d)} $ or, $ \lambda'_{222} $	1.0×10^{-5} $0.032 \cos \beta$	$[\tau \rightarrow e P^0 / \mu - e \text{ in nuclei}]$ [53]
$ \lambda'_{223} y_2^{(e)} $ or, $ \lambda'_{223} $	$7.6 \times 10^{-5} [\tilde{\nu}_{L_2}]^2$ $0.128 \cos \beta [\tilde{\nu}_{L_2}]^2$	$[B_s^0 \rightarrow e \bar{\mu}]$ [52]
$ \lambda'_{231} y_2^{(e)} ; \lambda'_{231} y_3^{(d)} $ or, $ \lambda'_{231} $	$1.3 \times 10^{-5} [\tilde{\nu}_{L_2}]^2; 1.6 \times 10^{-3} [\tilde{u}_{L_3}]^2$ $0.022 \cos \beta [\tilde{\nu}_{L_2}]^2; 0.099 \cos \beta [\tilde{u}_{L_3}]^2$	$[B_d^0 \rightarrow \mu \bar{e}]$ [52]
$ \lambda'_{232} y_2^{(e)} ; \lambda'_{232} y_3^{(d)} $ or, $ \lambda'_{232} $	$7.6 \times 10^{-5} [\tilde{\nu}_{L_2}]^2; 2.7 \times 10^{-4} [\tilde{u}_{L_3}]^2$ $0.128 \cos \beta [\tilde{\nu}_{L_2}]^2; 0.016 \cos \beta [\tilde{u}_{L_3}]^2$	$[B_s^0 \rightarrow \mu \bar{e}]$ [52]; $[b \rightarrow s \mu \bar{e}]$ [51]
$ \lambda'_{233} y_3^{(d)} $ or, $ \lambda'_{233} $	1.1×10^{-5} $6.8 \times 10^{-3} \cos \beta$	$[\tau \rightarrow e P^0 / \mu - e \text{ in nuclei}]$ [53]

Table 4: Some upper bounds on λ'_{2jk} ($j, k = 1, 2, 3$) couplings from various flavor-violating processes.

Starting with the λ couplings, we find the bounds in Table 3. We have only listed single coupling bounds, and those product ($\lambda \lambda$) bounds in which one of the couplings is a Yukawa coupling. This is because the Yukawa couplings are known up to $\tan \beta$, hence they provide the most robust bounds (however, we do consider the full set of constraints in our analysis). The λ' couplings are more numerous. Again, upper bounds exist on various products of the form $\lambda \lambda'$ and $\lambda' \lambda'$, and are listed in [21, 51–53]. As before, we describe the bounds on those products, one of which is a Yukawa coupling (either of the leptonic type or the down-type quark type). For some couplings, bounds exist from more than one experiment. We list the dominant bound in such cases, unless the bounds are comparable in which case we list all of them. The bounds for λ'_{2jk} and λ'_{3jk} are listed in Tables 4 and 5 respectively. As explained earlier, the bounds on λ_{i33} and λ'_{i33} ($i = 1, 2, 3$) are relaxed relative to those in standard RPV models. *In particular, the bound on λ'_{333} is very mild from Table 5; it can be comparable to the electroweak gauge couplings.* This can have an important effect on collider phenomenology related to the third generation (see Section 7).

In order to get a better idea about the constraints on these couplings, it is useful to understand what generic expectations we have for the spectrum of the model. This will be discussed more in Section 7;

Coupling(s)	Upper Bound(s)	Process
$ \lambda'_{311} y_3^{(e)} $ or, $ \lambda'_{311} $	$8.5 \times 10^{-5} [\tilde{\nu}_{L_3}]^2$ $8.47 \times 10^{-3} \cos \beta [\tilde{\nu}_{L_3}]^2$	$[\tau \rightarrow e \eta]$ [52]
$ \lambda'_{312} y_3^{(e)} $ or, $ \lambda'_{312} $	$9.7 \times 10^{-4} [\tilde{\nu}_{L_3}]^2$ $0.097 \cos \beta [\tilde{\nu}_{L_3}]^2$	$[\tau \rightarrow e K_s]$ [52]
$ \lambda'_{313} y_3^{(e)} $ or, $ \lambda'_{313} $	$3.7 \times 10^{-4} [\tilde{\nu}_{L_3}]^2$ $0.037 \cos \beta [\tilde{\nu}_{L_3}]^2$	$[B_d^0 \rightarrow e \bar{\tau}]$ [52]
$ \lambda'_{321} y_3^{(e)} $ or, $ \lambda'_{321} $	$9.7 \times 10^{-4} [\tilde{\nu}_{L_3}]^2$ $0.097 \cos \beta [\tilde{\nu}_{L_3}]^2$	$[\tau \rightarrow e K_s]$ [52]
$ \lambda'_{322} y_3^{(e)} $ or, $ \lambda'_{322} $	$4.6 \times 10^{-4} [\tilde{\nu}_{L_3}]^2$ $0.046 \cos \beta [\tilde{\nu}_{L_3}]^2$	$[\tau \rightarrow e \eta]$ [52]
$ \lambda'_{331} y_3^{(e)} $; $ \lambda'_{331} y_3^{(d)} $ or, $ \lambda'_{331} $	$3.7 \times 10^{-4} [\tilde{\nu}_{L_3}]^2$; $2.7 \times 10^{-3} [\tilde{u}_{L_3}]^2$ $0.037 \cos \beta [\tilde{\nu}_{L_3}]^2$; $0.168 \cos \beta [\tilde{u}_{L_3}]^2$	$[B_d^0 \rightarrow \tau \bar{e}]$ [52]
$ \lambda'_{333} y_3^{(d)} $ or, $ \lambda'_{333} $	2.1×10^{-2} $1.305 \cos \beta$	$[l_i \rightarrow 3 l_j]$ [53]

Table 5: Some upper bounds on λ'_{3jk} ($j, k = 1, 2, 3$) couplings from various flavor-violating processes. We do not show bounds on λ'_{323} and λ'_{332} as they do not appear in product bounds where the other coupling is a Yukawa coupling.

here we just make some brief remarks. We imagine a situation in which the (Dirac) gauginos are heavy and the scalars and Higgsinos are relatively light. For concreteness, we take $\mu = 200$ GeV, $m_L^2 \simeq m_E^2 \simeq (200 - 300 \text{ GeV})^2$, $M_1^D = 1000$ GeV, $M_2^D \simeq 1500$ GeV. The masses of the squarks are determined from current LHC constraints, which are studied in detail in the companion paper [1]. It turns out that the bounds on masses of the first two generation squarks are in the 600-700 GeV range, while the bounds on the third generation squark masses are lower, around 400 GeV.

With the above spectrum in mind, it is straightforward (although tedious) to check that (almost) all of the remaining bounds on the products of λ, λ' couplings in [21, 51–53] can be satisfied if the values of the λ, λ' couplings are assumed to saturate the bounds in Tables 3, 4 and 5. The exception is the following product bound:

Coupling(s)	Upper Bound	Process
$ \lambda_{231} \lambda'_{311} $	$2.1 \times 10^{-8} [\tilde{\nu}_{L_3}]^2$	$[\tau \rightarrow e P^0 / \mu - e \text{ in nuclei}]$ [53]

A simple choice, therefore, is to assume that the coupling λ'_{311} is negligible ($\simeq 0$), while all the other couplings still saturate the bounds in Tables 3, 4 and 5. We will see in Section 7 that this leads to rather interesting prospects for various signals such as lepto-quark-like signals, and single slepton/sneutrino production. Finally, it is worth mentioning that it is possible to make other (reasonable) ansätze about the flavor dependence of these couplings. In Appendix B, we discuss another simple ansatz about the flavor dependence of these couplings which allows a nice understanding of the relative magnitudes

of the various couplings and also satisfies existing constraints. It also has the advantage of *further* reducing the number of independent λ and λ' couplings.

6 The Scalar Electroweak Sector

In this section, we discuss some important features of the electroweak scalar sector of the model, and compare and contrast it with the well known case of the MSSM. This is of considerable importance, especially after the recent discovery of a Higgs-like particle near 125 GeV [2, 3]. A more thorough treatment of these issues, including the couplings of the Higgs-like particles in the model, will be the subject of another work [54].

From Eqs. (11) and (12), the electroweak scalar potential takes the form:

$$V^{EW} = V_F^{EW} + V_D^{EW} + V_{\text{soft}}^{EW} + V_{\text{loop}}^{(1)}, \quad (23)$$

$$V_F^{EW} = \sum_i \left| \frac{\partial W}{\partial \phi_i} \right|^2, \quad V_D^{EW} = \frac{1}{2} \sum_{a=1}^3 (D_2^a)^2 + \frac{1}{2} D_Y^2, \quad (24)$$

$$V_{\text{soft}}^{EW} = m_{H_u}^2 |H_u|^2 + m_{R_d}^2 |R_d|^2 + \sum_{i=1}^3 m_{\tilde{L}_i}^2 |\tilde{L}_i|^2 + m_s^2 |S|^2 + m_T^2 T^{a\dagger} T^a + t_s S + \frac{1}{2} b_S S^2 + \frac{1}{3} A_s S^3 + \frac{1}{2} b_T T^a T^a + B \mu_L^{(i)} H_u L_i + A_T S T^2 + A_S^{(i)} S H_u L_i + A_T^{(i)} H_u T L_i + \text{h.c.},$$

while $V_{\text{loop}}^{(1)}$ refers to the one-loop contribution to the effective potential, which will be specified below. Here i runs over all the electroweak scalar fields which could receive *vev*'s, and D_Y and D_2^a are the hypercharge and $SU(2)_L$ D -terms, respectively. Compared to the MSSM case, the D -terms contain additional pieces associated with the $SU(2)_L$ and $U(1)_Y$ adjoint fields:

$$D_2^a = g(H_u^\dagger \tau^a H_u + R_d^\dagger \tau^a R_d + \tilde{L}_i^\dagger \tau^a \tilde{L}_i + T^\dagger \lambda^a T) + \sqrt{2} (M_2^D T^a + \text{h.c.}), \quad (25)$$

$$D_Y = \frac{g'}{2} (H_u^\dagger H_u - R_d^\dagger R_d - \tilde{L}_i^\dagger \tilde{L}_i) + \sqrt{2} (M_1^D S + \text{h.c.}),$$

where τ^a and λ^a are the two and three-dimensional $SU(2)$ generators respectively. Note that the D terms above give rise to new *trilinear* couplings in the scalar potential. Also, the masses of the real and imaginary parts of $S = S_R + i S_I$ and $T = T_R + i T_I$ are split in Eq. (23). For instance, if M_i^D , b_S and b_T are real, then $m_{S_R}^2 = m_s^2 + b_S + 4(M_1^D)^2$ and $m_{S_I}^2 = m_s^2 - b_S$ while $m_{T_R}^2 = m_T^2 + b_T + 4(M_2^D)^2$ and $m_{T_I}^2 = m_T^2 - b_T$. For simplicity, we assume that there are no CP-violating phases in the potential.

In order to minimize the above potential, we point out some important simplifications. First, EW precision constraints on the ρ -parameter require the triplet Higgs *vev*, $\langle T^3 \rangle \equiv v_T$, to be small ($\lesssim 3$ GeV [55]), which is naturally achieved if the triplet soft breaking mass $m_T \gtrsim \text{TeV}$. Therefore, the effect of the triplet on the minimization of the potential must be small, and v_T can be set to zero in the first approximation. Second, since the R -symmetry forbids the term $B \mu H_u R_d$, it is easy to see that $\langle R_d \rangle = 0$ if $m_{R_d}^2 > 0$, i.e. there is no spontaneous breaking of the $U(1)_R$ symmetry. Also, because

R_d has a different R -charge ($= 2$) than the rest of the electroweak fields ($= 0$), the degrees of freedom in R_d do not mix with those in the other fields and decouple from the rest.

It is important to understand the similarities and differences in the structure of the scalar potential relative to that in “supersoft” SUSY breaking studied in [28]. Since the gauge sector of the model is similar to that in [28], the model shares the good feature that unlike the MSSM, the usual logarithmic divergence from the stop contributions to the Higgs mass-squared parameter $m_{H_u}^2$ are cutoff by the Dirac gluino mass, leading to only a *finite* contribution. Thus, in contrast to the MSSM, a Dirac gluino mass in the multi-TeV range is consistent with electroweak-naturalness.

On the other hand, the matter sector of the model is rather different from that in [28]. Indeed, in the latter case one gets a vanishing D -term contribution to the Higgs quartic coupling at tree level, which is obviously not a good starting point to obtain a Higgs mass near 125 GeV. In our model, however, the above conclusion is circumvented by the presence of soft (but not supersoft) operators arising from F -terms of the X spurion in (6) which yield the soft parameters $\{m_s^2, m_T^2, b_S, b_T\}$, etc. Also, the presence of the superpotential couplings in (11) proportional to λ_u^S and λ_u^T can give rise to new F -term contributions to the Higgs quartic coupling at tree level if R_d gets a vev , as in [56, 57]. However, since in our model $\langle R_d \rangle = 0$, this tree-level F -term contribution is not present. Nevertheless, the λ_u^S and λ_u^T couplings do provide important contributions to the Higgs quartic coupling at loop level. We will see in the next subsection that this is very important in obtaining a CP-even mass eigenstate with mass ~ 125 GeV.

With the above simplifications, it suffices to minimize the scalar potential with respect to the neutral fields - $\{H_u^0, \tilde{\nu}_{(a)}, S_R\}$ to study electroweak symmetry breaking (EWSB):¹⁴

$$\begin{aligned}
0 &\simeq \mu^2 + m_{H_u}^2 - \left(\frac{g^2+g'^2+4\delta\lambda_u}{4}\right) v^2 c_{2\beta} + \left(\frac{2\delta\lambda_u+\delta\lambda_3}{2}\right) v^2 c_\beta^2 + \sqrt{2}g'v_s M_1^D + \lambda_u^S v_s (2\mu + \lambda_u^S v_s) + t_\beta^{-1} B\mu_L^{(a)}, \\
0 &\simeq m_{\tilde{L}(a)}^2 + \frac{(g^2+g'^2-\delta\lambda_3+2\delta\lambda_\nu)}{4} v^2 c_{2\beta} + \left(\frac{\delta\lambda_3+2\delta\lambda_\nu}{4}\right) v^2 - \sqrt{2}g'v_s M_1^D + t_\beta B\mu_L^{(a)}, \\
0 &\simeq [m_{S_R}^2 + (\lambda_u^S)^2 v^2 s_\beta^2] v_s - \frac{g'}{\sqrt{2}} M_1^D v^2 c_{2\beta} + (t_S + \lambda_u^S \mu v^2 s_\beta^2).
\end{aligned} \tag{26}$$

Here, s_β stands for $\sin \beta$ and so on, and $\{\delta\lambda_u, \delta\lambda_\nu, \delta\lambda_3\}$ denote the dominant radiative corrections to the quartic terms: $\frac{1}{2}\delta\lambda_u (|H_u^0|^2)^2$, $\frac{1}{2}\delta\lambda_\nu (|\tilde{\nu}_{(a)}|^2)^2$ and $\frac{1}{2}\delta\lambda_3 |H_u^0|^2 |\tilde{\nu}_{(a)}|^2$ respectively. In the limit where λ_u^S is negligible, the leading-logarithm contributions to these radiative corrections are given by [56]:

$$\begin{aligned}
\delta\lambda_u &\simeq \frac{3y_t^4}{16\pi^2} \log\left(\frac{m_{\tilde{t}_1} m_{\tilde{t}_2}}{m_t^2}\right) + \frac{5(\lambda_u^T)^4}{16\pi^2} \log\left(\frac{m_T^2}{v^2}\right), \\
\delta\lambda_\nu &\simeq \frac{3y_b^4}{16\pi^2} \log\left(\frac{m_{\tilde{b}_1} m_{\tilde{b}_2}}{m_t^2}\right) + \frac{5(\lambda_u^T)^4}{16\pi^2} \log\left(\frac{m_T^2}{v^2}\right), \\
\delta\lambda_3 &\simeq \frac{5(\lambda_u^T)^4}{32\pi^2} \log\left(\frac{m_T^2}{v^2}\right),
\end{aligned} \tag{27}$$

where the renormalization scale is taken to be close to the electroweak vev . The trilinear soft terms A_s, A_s^i have been neglected here since they can be suppressed for reasons mentioned below (6). In the

¹⁴For numerical results we do a full analysis, including all vev 's, and based on the full Coleman-Weinberg potential.

above approximation, the CP-even and the CP-odd neutral Higgs fields are linear combinations of the real and imaginary parts of $\{H_u^0, \tilde{\nu}_L, S\}$ respectively. The charged Higgs H^+ , on the other hand, is a combination of $\{H_u^+, \tilde{e}_L^\dagger\}$.

6.1 The ~ 125 GeV Eigenstate

It is important to understand what region of parameter space of the model gives rise to an eigenstate with mass near 125 GeV, given the recent discovery of a Higgs-like particle with that mass. We will only make some general and somewhat qualitative comments, leaving a detailed study of these issues for future work [54].

To start, let us write down the tree level ($\delta\lambda_u = \delta\lambda_\nu = \delta\lambda_3 = 0$) mass matrix for the CP-even neutral states in the $(H_u^0, \tilde{\nu}_{(a)}, S_R)$ basis:

$$\mathcal{M}_H^2 = \begin{pmatrix} \frac{1}{2}[(g^2 + g'^2)v^2 s_\beta^2 - 2t_\beta^{-1} B\mu_L^{(a)}] & [-\frac{(g^2+g'^2)}{4}v^2 s_{2\beta} + B\mu_L^{(a)}] & v s_\beta [\sqrt{2}g' M_1^D + 2\lambda_u^S(\mu_u + \lambda_u^S v_s)] \\ [-\frac{(g^2+g'^2)}{4}v^2 s_{2\beta} + B\mu_L^{(a)}] & \frac{1}{2}[(g^2 + g'^2)v^2 c_\beta^2 - 2t_\beta B\mu_L^{(a)}] & -\sqrt{2}g'v c_\beta M_1^D \\ v s_\beta [\sqrt{2}g' M_1^D + 2\lambda_u^S(\lambda_u^S v_s + \mu_u)] & -\sqrt{2}g'v c_\beta M_1^D & \frac{-2(t_s + \lambda_u^S \mu_u v^2 s_\beta^2) + \sqrt{2}g'v^2 c_{2\beta} M_1^D}{2v_s} \end{pmatrix}$$

where we have used the minimization conditions in (27) to get rid of the non-holomorphic soft mass-squareds for $H_u^0, \tilde{\nu}_{(a)}$ and S .

By inspection, one can see that the mixing angle between S_R and $\{H_u^0, \tilde{\nu}_{(a)}\}$ is essentially controlled by the ratio v_s/v . Hence, a larger v_s will make this mixing angle larger, pushing down the lightest eigenvalue due to ‘‘eigenvalue-repulsion’’. Thus, v_s should be small in order to maximize the lightest eigenvalue (we do not consider the possibility of a very light singlet scalar). In this limit where the off-diagonal entries are relatively small, it is then not hard to see that the largest eigenvalue is predominantly S_R , while the $H_u^0 - \tilde{\nu}_{(a)}$ block gives rise to a tree-level smallest eigenvalue approaching that in the MSSM.

Thus, in order to obtain the lightest CP-even Higgs mass around 125 GeV, a reasonably large radiative contribution to the Higgs quartics (primarily $\delta\lambda_u$) is required.¹⁵ However, unlike the MSSM,

¹⁵As explained earlier, in this model there are no additional *tree level* contributions proportional to $(\lambda_u^S)^2$ or $(\lambda_u^T)^2$, unlike that in [56, 57].

Benchmark I	Benchmark II
$\tan \beta = 3$	$\tan \beta = 17$
$\lambda_u^S = 0.1$	$\lambda_u^S = 0.1$
$\lambda_u^T = 1.0$	$\lambda_u^T = 0.9$
$\mu_u = 200$ GeV	$\mu_u = 200$ GeV
$M_1^D = 200$ GeV	$M_1^D = 200$ GeV
$M_2^D = 1000$ GeV	$M_2^D = 1000$ GeV
$B\mu_L \simeq -(174 \text{ GeV})^2$	$B\mu_L \simeq -(123 \text{ GeV})^2$
$t_S \simeq (174 \text{ GeV})^3$	$t_S \simeq (138 \text{ GeV})^3$
$m_{S_R}^2 \simeq (1115 \text{ GeV})^2$	$m_{S_R}^2 \simeq (880 \text{ GeV})^2$
$m_T^2 \simeq (1450 \text{ GeV})^2$	$m_T^2 \simeq (1390 \text{ GeV})^2$
$m_{\tilde{t}_1}^2 = m_{\tilde{t}_2}^2 = (500 \text{ GeV})^2$	$m_{\tilde{t}_1}^2 = m_{\tilde{t}_2}^2 = (500 \text{ GeV})^2$
$m_h \simeq 125$ GeV	$m_h \simeq 125$ GeV

Table 6: Two benchmarks giving rise to a lightest CP-even Higgs mass close to 125 GeV. We take $v_s = -5$ GeV in both cases.

where the dominant contribution to $\delta\lambda_u$ is provided by the stop squarks, here the adjoints S and T can also provide a significant contribution through terms proportional to λ_u^S and λ_u^T in (11). In fact, it is possible that the bulk of the radiative contribution is provided by the triplets T in the loop, with λ_u^S small and λ_u^T close to unity [see the approximate expressions for $\{\delta\lambda_u, \delta\lambda_\nu, \delta\lambda_3\}$ in (27)]. We give two benchmark examples¹⁶ in Table 6 with values of the important parameters and for two choices of $\tan\beta$, close to the minimum and maximum values in (22). In these benchmark examples, the stop squarks are taken to be around 500 GeV, so the dominant radiative correction is provided by the triplet T . It turns out that even though the singlet and triplet scalar masses are \gtrsim TeV, the sensitivity of the Higgs potential on them is *less* than that on heavy stops in the MSSM which could generate a ~ 125 GeV Higgs mass, making this model significantly less fine-tuned than the MSSM. Part of the reason is to be found in the factor of 5 versus 3 displayed in (27), which makes the contribution to the Higgs quartic more effective for the triplets than for the stops. For instance, for $y_t = \lambda_u^T$, a 500 GeV (1 TeV) triplet gives the same contribution to $\delta\lambda_u$ as stops with $m_{\tilde{t}_1} = m_{\tilde{t}_2} = 1$ TeV ($m_{\tilde{t}_1} = m_{\tilde{t}_2} = 3.2$ TeV). In addition, one finds that the radiative correction of the triplet to $m_{H_u}^2$ corresponds to that of a *single* stop with $m_{\tilde{t}_i}^2 = m_T^2$ and $y_t = \lambda_u^T$. Hence, for fixed $\delta\lambda_u$ and equal stop masses (no stop LR mixing), one can estimate an overall suppression of the triplet “quadratic divergence” compared to that of the stops by a factor of about

$$\frac{\Delta m_{H_u}^2|_{\text{triplet}}}{\Delta m_{H_u}^2|_{\text{stops}}} \sim \frac{1}{2} \frac{(\lambda_u^T)^2}{y_t^2} \frac{e^{\frac{16\pi^2\delta\lambda_u}{5(\lambda_u^T)^4}}}{e^{\frac{16\pi^2\delta\lambda_u}{3y_t^4}}} . \quad (28)$$

For $\lambda_u^T \approx 1$ and $m_T \approx 1$ TeV (corresponding to $\delta\lambda_u \approx 0.11$), the above represents a suppression by a factor of about 20, which results in a significant reduction in fine-tuning. We have checked that the fine-tuning can indeed be mild by computing the logarithmic derivatives of the EW scale w.r.t. the microscopic parameters, in the framework of the 1-loop effective potential.¹⁷ Remember also that, as mentioned earlier, the Higgs potential is much less sensitive to the (Dirac) gluino mass in this model, compared to the (Majorana) gluino mass in the MSSM.

It is also interesting to note that a combined global fit to Higgs properties, $\text{Br}(B \rightarrow X_s \gamma)$, and the W -mass, show a preference for 400-500 GeV degenerate stops, provided there is an additional mechanism to obtain a ~ 125 GeV Higgs eigenstate [58]. This is precisely the situation in the benchmark examples in Table 6, where the triplet provides the additional contribution to the Higgs mass (its heaviness being motivated by EWPT). Finally, note that since the couplings $\{\lambda_u^S, \lambda_u^T\}$ grow with energy and since λ_u^T is close to unity in Table 6, one finds¹⁸ a Landau pole at around 10^7 GeV (10^8 GeV) for Benchmark I (Benchmark II), implying that additional new physics has to come in around those scales. This is consistent with our approach specified in the Introduction; we are primarily interested in understanding the nature of physics affecting the LHC, and are agnostic about effects at higher energy scales. Presumably a microscopic understanding of supersymmetry breaking within this

¹⁶We have used the full Coleman-Weinberg one-loop effective potential to compute the lightest CP-even Higgs mass eigenvalue.

¹⁷We will present our results in more detail in [54].

¹⁸We have computed the RGE’s by implementing the full model in SARAH [59, 60].

setup¹⁹ will provide insights into the nature of physics at such scales.

Before moving on to discussing various aspects of collider phenomenology, it is worth commenting on the properties of the ~ 125 GeV eigenstate within the model. For the two benchmarks, it can be readily checked that this state is primarily a combination of H_u^0 and $\tilde{\nu}_{(a)}$ with only a negligible S_R component. Thus, this state has properties very similar to the lightest CP-even state arising within the MSSM (with $\tilde{\nu}_{(a)}$ replaced by H_d^0 of course). As mentioned at the beginning of the section, the couplings, production, and decays of this and the other scalar electroweak states will be studied in detail in another work [54].

7 Phenomenology

In this section, we discuss several phenomenological features of the framework in which lepton number is related to the R -symmetry ($R = R_1$). Since the phenomenology of this class of models is rather novel, in this paper we only outline the *broad* phenomenological consequences of the framework for collider and neutrino physics. A detailed treatment of these issues is provided in a companion paper [1], which studies the existing collider constraints on this class of models, as well as the various interesting signals which could be probed in the near future.

The main qualitative features of the phenomenology of this class of models which sets it apart from traditional supersymmetric models like the (R -parity conserving) MSSM (or many of its cousins like the NMSSM or models with extra vector-like matter²⁰), are the following:

- The existence of a “Dirac” structure in the gauge sector of the model. Among other things, this gives rise to a suppression of the production of squark pairs at the LHC compared to the Majorana case, which helps in relaxing the bounds on superpartners from current searches [1]. Another straightforward consequence of this is a suppression of those signals which depend on the *Majorana* nature of gluinos, e.g. same-sign (SS) dileptons.
- The R -symmetry dictates a specific set of operators in the superpotential and $\mathcal{L}_{\text{soft}}$, distinct from the “standard” cases. In particular, in the $R = R_1$ realization, there exist “RPV” operators of the type $\lambda_{ijk} L_i L_j E_k^c$ and $\lambda'_{ijk} L_i Q_j D_k^c$ in the superpotential, and $B\mu_L^{(i)} H_u L_i$ in the soft Lagrangian. Since these operators are consistent with the R -symmetry (hence with lepton number), they cannot generate neutrino masses. Therefore, the sneutrino can have a significant vev in these models, thereby acting as a genuine Higgs field, in stark contrast to standard RPV models.

Also, since the usual trilinear terms involving squark, slepton and Higgs fields are forbidden, there is no left-right mixing in the squark and slepton scalar mass-squared matrices.

- The existence of a sizeable (electron) sneutrino vev implies that some of the λ and λ' couplings are the lepton and down-type Yukawa couplings, respectively (which are well known up to $\tan\beta$). As explained in Sections 3 and 5, this implies that the flavor structure of the λ and λ' couplings,

¹⁹At present, we have only done a spurion analysis of supersymmetry breaking, in Section 2.1.

²⁰These are some of the popular models which could also give rise to Higgs mass near 125 GeV without much tuning.

as well as the various indirect constraints on these, are rather specific compared to standard RPV models.

Furthermore, it implies that there is mixing between the neutrino(s) and neutralinos, and between the electron and the charginos, but with a different dependence on the parameters compared to that in standard RPV models, as explained in Section 3.

A rich and interesting pattern of signatures results from such a structure. For example, decays of the “LSP”²¹ like $\tilde{X}_1^{0+} \rightarrow Z\bar{\nu}_e, h\bar{\nu}_e, W^- e_L^+$, and $\tilde{\tau}_L^- \rightarrow \tau_R^- \bar{\nu}_e, \bar{t}_L b_R$ are prompt and have a significant branching ratio, unlike standard RPV models.

- The existence of an R -symmetry²² implies the conservation of two charges, the electric charge and the R -charge, even after electroweak symmetry breaking. In particular, the neutralinos and charginos are Dirac in nature, and their interactions must conserve both charges (see Sections 4.1 and 4.2). This gives rise to a rich and interesting pattern of decays of the neutralinos and charginos, and sleptons and squarks, which is different from that in the MSSM.
- In principle, flavor physics can be quite rich as well since bounds from flavor-violating processes are quite relaxed with an R -symmetry [29]. However, we will not consider this in detail in this work.

Although different subsets of the above set of signals can be mimicked by other models, the entire set of signals is rather unique. Hence, if the model is correct, it should be possible to distinguish this class of models from other models in the near future (more about this in Sections 7.3 and 7.5).

Before going into more details about the phenomenology, it is useful to have an understanding of the spectrum of the model. Since the motivation is to build an electroweak-natural model, we consider a situation in which the third generation squarks are light ($\lesssim 500$ GeV). In fact, as will be shown in [1], the bounds on third generation squarks are weaker than 500 GeV, while that on the first and second generation squarks also turn out to be mild – in the range 600-700 GeV. This bound assumes a heavy Dirac gluino ($M_3^D \simeq 2$ TeV), which is still consistent with naturalness due to the existence of a “supersoft” structure in the gauge interactions of the model [28]. The Dirac wino is expected to be heavy (\gtrsim TeV) to satisfy electroweak precision measurements of the coupling of the Z to charged leptons for a reasonably large range of the sneutrino vev (see Section 5). For concreteness we take $M_2^D \simeq 1.5$ TeV. There are no direct bounds on the Dirac bino; however anticipating that the origin of its mass is tied to those of the wino and gluino, we take $M_1^D \simeq 1$ TeV for concreteness.²³ Since the μ parameter is directly connected to naturalness, we take it around the EW scale, $\mu \simeq 200$ GeV. This

²¹“LSP” here stands for the *lightest non SM-like superpartner which is charged under the SM*. The “LSP” is really unstable, just as in RPV models. Note that the qualification of being charged under the SM is relevant because the gravitino can be the lightest BSM particle in many cases; however, in our framework, final states that include a gravitino have a negligible branching fraction and play no role in collider physics, *unlike* that in gauge mediation (see Section 7.5). Hence, we will reserve the term “LSP” for the lightest non SM-like superpartner charged under the SM, such as a neutralino or stau. This is phenomenologically useful since the “LSP” is the last step of the SUSY decay chains before producing a pure SM final state.

²²It is assumed to be (explicitly) broken only by a very small amount, so for collider purposes the symmetry is exact.

²³In Section 6.1, we have taken $M_1^D = 200$ GeV, but a CP-even Higgs near 125 GeV is also possible with $M_1^D = 1$ TeV.

implies that the lightest non SM-like²⁴ charginos and neutralinos are mostly Higgsino-like. Finally, the sleptons are expected to be among the lightest particles in the BSM spectrum because of the close connection of the slepton sector with EWSB in our framework. Furthermore, a good degree of degeneracy among the three generations of sleptons is expected. Since the electron sneutrino plays the role of the down-type Higgs, electroweak naturalness requires its soft mass to be close to the electroweak scale. For concreteness, we take $m_L^2 \simeq m_{\bar{E}}^2 \simeq (200 - 300 \text{ GeV})^2$ for all three generations. Thus, the lightest BSM particles consist of the sleptons, sneutrinos and Higgsino-like neutralinos and charginos. Depending on the situation, either the sleptons/sneutrinos or the Higgsino-like neutralino could be the “LSP”.

7.1 Summary of Bounds from Existing Searches

In Ref. [1] we perform a more detailed analysis of the implications for the LHC of the leptonic $U(1)_R$ symmetry. We highlight here a subset of those findings. In the LHC context, the small R -violating effects can be neglected, and the physics effectively exhibits a new conserved quantum number, the R -charge. As described above, we focus on the region of parameter space where the Dirac gaugino masses are in the 1 – 2 TeV range, which effectively decouples (in a first approximation) the bino-singlino, wino-tripletino and gluino-octetino Dirac states (though the latter can have some impact on squark pair-production through certain t -channel diagrams). As a result the lightest (higgsino-like) neutralino and chargino states play an important role, through the decays listed in the third item above. Such decay channels are also intimately related to the fact that down-type fermions get their masses from a sneutrino vev . We note that, due to its higgsino-like nature and the typical branching fractions, the LEP bounds on charginos are still stronger than those available at the LHC [61], in our framework.

Let us start by summarizing the results of the interpretation of the current ATLAS and CMS searches on the first and second generation squarks within the leptonic $U(1)_R$ model. The first point to notice is that, as emphasized in [22, 23], the Dirac nature of the gluino results in a suppression of the squark pair-production cross section.²⁵ By allowing for lighter squarks than in the MSSM, there is an important secondary consequence that compounds this effect. Namely, that the efficiencies of the current searches, which are optimized for MSSM-like production cross sections, can be significantly reduced due to the aggressiveness of the present cuts. The upshot is that squarks as light as 600 – 700 GeV can be consistent with the various generic SUSY searches (involving jets, varying number of leptons and \cancel{E}_T), to be compared to the current limit of 1.4 TeV in the MSSM (when the gluinos are heavy) [62].

We also find that within our framework the bulk of the processes end up producing some amount of missing energy (in the form of neutrinos), so that most of the present search strategies can apply with minor modifications. However, there are some topologies involving only visible particles (for instance

²⁴Note that since the neutrino(s) and the electron mix with the neutralinos and charginos respectively, technically *these* are the lightest neutralino(s) and chargino, respectively.

²⁵The Dirac gluino pair-production cross section is larger than in the MSSM, but for decoupled squarks the current bounds on the gluino mass are only slightly stronger than for the Majorana case due to the steeply falling cross section with the Dirac gluino mass. In any case, we are taking gluinos at around 2 TeV to emphasize that a spectrum with squarks lighter than gluinos is fairly natural in our framework.

when the neutralinos decay through their We channel, with a hadronically decaying W). It would be interesting to design search strategies for such “no \cancel{E}_T ” channels. Another important example of no missing energy channel is the lepto-quark one. Interestingly, the RH strange squark has a sizable branching fraction into $\tilde{s}_R \rightarrow e_L^- j$. Current LQ searches have only a slightly smaller reach than the generic SUSY searches above (the latter assume degenerate squark masses), and a discovery in such a channel represents an exciting possibility. Besides allowing for a measurement of the LQ mass, such decay modes may allow to extract additional information from “mixed topologies”, where one of the pair produced particles decays visibly through their lepto-quark mode, while the other one decays into states involving missing energy, which can be used for triggering and background reduction. One example of this sort is described in Subsection 7.4, and illustrates how one may infer that the sneutrino vev is indeed large, a characteristic of the leptonic R -symmetry. Other examples are presented in [1].

The third generation is likely of central importance for understanding the physics of EWSB. As was emphasized in Section 6.1, the stops can be reasonably expected to lie in the few hundred GeV range, based on naturalness considerations, since the bulk of the lightest CP-even Higgs mass arises instead from the radiative corrections of a heavy triplet (with moderate associated fine-tuning). As it turns out, the lepto-quark nature of \tilde{t}_L , \tilde{b}_L and \tilde{b}_R offers a powerful handle into this sector. As further explained in the companion paper [1], depending on the sneutrino vev , such searches can easily cover the interesting expected range. Still, at present, the strongest constraint arises from the CMS direct sbottom search [63], which can be interpreted as leading to a sneutrino- vev -dependent bound on \tilde{b}_L that varies between ~ 300 and 500 GeV, for representative values of the model parameters. The same search results in a bound on the RH sbottom of close to 500 GeV. The LH sbottom bound implies indirectly a lower bound on the LH stop a few tens of GeV larger, since due to the absence of LR mixing, the stop is always heavier than the sbottom. We therefore see that a large part of the interesting mass range has been tested, and that naturalness would lead us to conclude that a discovery should be possible in the relatively near future. We discuss a further interesting feature of a possible LQ signal in Section 7.3. One should also mention that most of the current dedicated searches for third generation squarks do not apply in a straightforward manner, but it should be possible to adapt them to cover more general possibilities than found in simple limits of the MSSM phenomenology.

7.2 Resonant Slepton/Sneutrino Production

One of the characteristic features of the presence of the $\lambda'_{ijk} L_i Q_j D_k^c$ operator is the resonant production of sleptons and sneutrinos, similar to that in RPV models. In this subsection, we would like to study the prospects for resonant slepton/sneutrino production at the LHC, *assuming* that the bounds on the λ and λ' couplings in Tables 3, 4 and 5 are saturated. As explained in Section 5, the sole exception is the λ'_{311} coupling, which we assume to be negligible ($\simeq 0$). Furthermore, for simplicity we will study the simple case where the sleptons and sneutrinos are the “LSP”, so that the only decay modes of the slepton/sneutrino are via the λ and λ' couplings (resonant production occurs via λ' couplings). Finally, we organize our analysis in terms of the two-body final states coming from slepton/sneutrino decays. For a given final state, we assume that only those λ and λ' couplings which could give rise to that particular final state are non-zero and that they saturate the bounds in Section 5. For example, for the

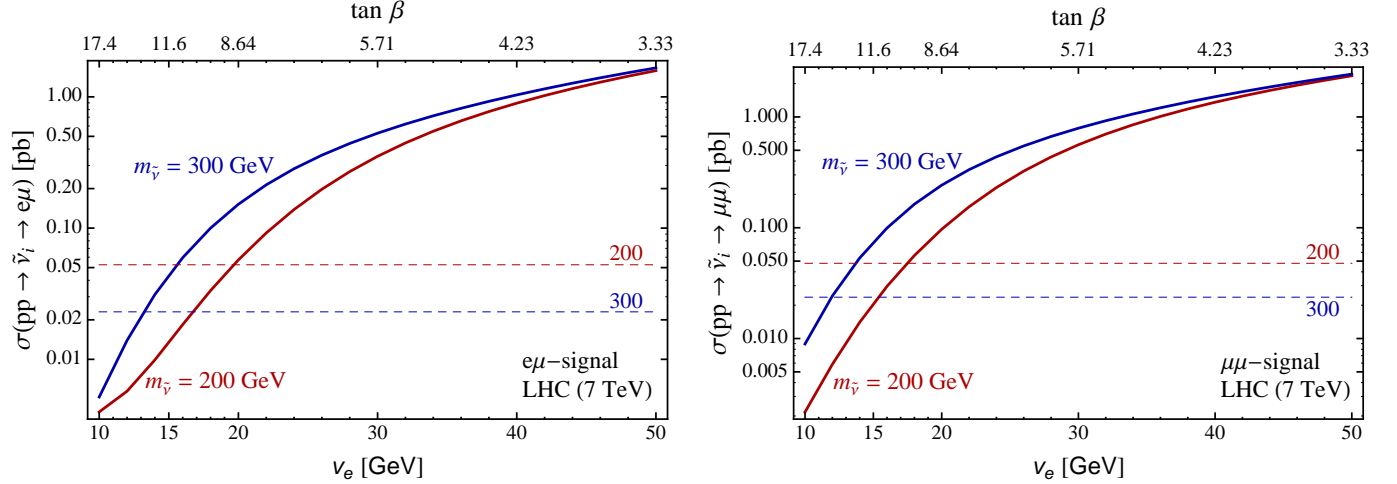


Figure 2: Upper bounds on $\sigma_{prod} \times BR$ for the $e^\pm \mu^\mp$ (left panel) and $\mu^+ \mu^-$ (right panel) final states as a function of the electron sneutrino v_{ev} for two different values of the sneutrino masses: 200 GeV and 300 GeV. For $e^\pm \mu^\mp$, both $\tilde{\nu}_\mu$ and $\tilde{\nu}_\tau$ are produced, and the non-vanishing couplings are taken to be $(\lambda'_{211}, \lambda'_{222}, \lambda'_{311}, \lambda'_{322})$ for production and $(\lambda_{212}, \lambda_{231})$ for decay. For $\mu^+ \mu^-$, only $\tilde{\nu}_\tau$ is produced, and the non-vanishing couplings are taken to be $(\lambda'_{311}, \lambda'_{322})$ for production and (λ_{322}) for decay. The λ and λ' couplings identified with lepton and down-type Yukawa couplings are always present. The LHC bounds are shown as dashed lines. These bounds are provided by [64] for $e^\pm \mu^\mp$ and by [65] for $\mu^+ \mu^-$.

$e^\pm \mu^\mp$ final state, this would imply that the production of both $\tilde{\nu}_\mu$ and $\tilde{\nu}_\tau$ is considered turning on those couplings which allow them to be produced $(\lambda'_{211}, \lambda'_{222}, \lambda'_{311}, \lambda'_{322})$, and those which allow them to decay to $e^\pm \mu^\mp$ $(\lambda_{212}, \lambda_{231})$. Of course, the λ and λ' couplings which are identified with the lepton Yukawa $(\lambda_{122}, \lambda_{133})$ and down-type Yukawa $(\lambda'_{111}, \lambda'_{122}, \lambda'_{133})$ couplings are always assumed to be present and non-vanishing.²⁶

Comparing with the existing experimental bounds from the various two-body final states from the Tevatron and the LHC, we find that only the $e^\pm \mu^\mp$ and $\mu^+ \mu^-$ final states provide constraints on the parameter space. Fig. 2 shows the bounds on the $\sigma_{prod} \times BR$ as a function of the (electron) sneutrino v_{ev} (varied within the allowed range) for the $e^\pm \mu^\mp$ and $\mu^+ \mu^-$ final states. One finds that only values of the sneutrino v_{ev} close to the minimum value (maximum for $\tan \beta$) are allowed by the current LHC constraints. However, since these bounds are for values of couplings *saturating* the bounds in Section 5, this simply suggests that there are good detection prospects for these final states in the future, within this framework.

7.3 Lepto-quark (LQ) Signals – R -symmetry at the TeV Scale

Another important consequence of the $\lambda'_{ijk} L_i Q_j D_k^c$ operator is the presence of lepto-quark (LQ) signals. Again, since the LQD^c operator is also present in standard RPV models, these signals are present in principle in RPV models as well. However, we will argue below that observation of certain LQ signals will in fact suggest the existence of an R -symmetry in the TeV scale Lagrangian, which is, furthermore,

²⁶Note that we assume that if more than one sneutrino or slepton species can lead to the given final state, they have comparable masses but are split by an amount larger than their width, so that interference effects are negligible. This is well justified since the widths of the sneutrinos/sleptons are expected to be extremely small.

tied to lepton number ($R = R_1$). This is made possible by a connection to neutrino physics, as will be explained. Finally, we will mention a number of situations in which further information from other channels would be required in order to rule out alternative interpretations. Fortunately, such information should be accessible at the LHC if the leptonic $U(1)_R$ symmetry is indeed at play.

Because squarks have R -charge 1 in the model, they also carry lepton-number since it is identified with the R -symmetry ($R = R_1$). These scalar “lepto-quarks” are pair produced by QCD interactions, but can decay via the λ' coupling above, thereby displaying their LQ nature. Such channels can be very important for the third generation²⁷ for two reasons – i) the bounds on λ'_{333} are quite weak from Section 5, and ii) the third generation Yukawa couplings²⁸ are the largest, while the third generation squarks can naturally be the lightest. In particular, this means that λ'_{133} and λ'_{333} can be $\mathcal{O}(1)$, and could give rise to the decays

$$\begin{aligned} \tilde{t}_L &\rightarrow b_R l_L^+ , & \tilde{b}_R &\rightarrow t_L l_L^- , & l_L &= e_L, \tau_L , \\ \tilde{b}_L &\rightarrow b_R \bar{\nu} , & \tilde{b}_R &\rightarrow b_L \nu , & \nu &= \nu_e, \nu_\tau , \end{aligned} \quad (29)$$

plus their conjugate processes. Since for an electroweak-natural model we expect the third generation squarks to have masses $\lesssim 500$ GeV, there are good prospects of observing these signals. The observation of the LQ signal (29) may provide support for the existence of the $U(1)_R$ symmetry in the full Lagrangian at the TeV scale, which is a stronger conclusion than the one one could reach based on the observation of Dirac gluino signatures alone. The argument is the following.

Let us start by assuming that some of the LQ signals (29) have been observed [either from \tilde{b}_R or from the $(\tilde{t}_L, \tilde{b}_L)$ doublet]. Although it may be hard to distinguish the decays in the second line in (29) from the “standard” SUSY decays involving a (massive) neutralino instead of the neutrino, the simultaneous observation of the (fully visible) decays involving a charged lepton may be taken, based on $SU(2)_L$ invariance, as indication that (at least part of) the missing energy signal is associated with a neutrino. We will also assume that the observed LQ is indeed a *third generation* squark (as opposed to first/second generation), and will further comment on this assumption below.

Given the above LQ observation, it is possible to obtain a surprisingly large amount of information regarding the structure of the soft supersymmetry breaking terms. This is because the LQD^c operators lead to a contribution to the neutrino masses given by:

$$\Delta m_{\nu_i} \sim \frac{3(\lambda'_{i33})^2 m_{\text{LR}}^2}{16\pi^2 m_b^2} m_b , \quad i = 1, 2, 3 , \quad (30)$$

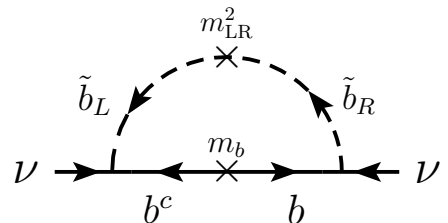


Figure 3: Contribution to the neutrino mass from a SUSY lepto-quark.

where m_{LR}^2 is the left-right mixing in the sbottom mass-squared matrix. Note that in the R -symmetric limit this left-right mixing is forbidden, but it is present in RPV models in general. For an electroweak-natural model, barring fine-tuned cancellations amongst several contributions, there are two ways in

²⁷The RH strange squark can also display interesting LQ decay channels, see [1].

²⁸Recall that when $R = R_1$, the couplings λ_{1jj} , $j = 2, 3$, and λ'_{1kk} , $k = 1, 2, 3$, are identified with the lepton and down-type Yukawa couplings, respectively.

which Eq. (30) can be consistent with the upper bound on neutrino masses: *i*) a suppressed coupling λ'_{i33} , or *ii*) a suppressed m_{LR}^2 .

In RPV models, where typically $m_{\text{LR}}^2 = m_b(A_b - \hat{\mu} \tan \beta) \sim \mathcal{O}(m_b m_{\bar{b}})$, this would imply situation (i) - a very suppressed coupling λ'_{i33} ($\lesssim 10^{-3}$). Here $\hat{\mu}$ denotes the traditional “ μ -term”.²⁹ However, the observation of a LQ signal with a very suppressed λ'_{i33} coupling is only possible for a *rather special* situation, i.e. when the LQ decay channel (controlled by λ'_{i33}) of the relevant squark (sbottom here) has a significant branching ratio (BR) in spite of λ'_{i33} being very suppressed. We will discuss cases in Section 7.3.1 when this special situation is satisfied. In a typical situation, however, one expects at least some neutralinos and/or charginos to be lighter than the third generation squarks (which could have masses $\sim 400 - 500$ GeV). This is also motivated by electroweak-naturalness, where a natural solution of the EWSB minimization conditions typically requires $\mu \lesssim 200 - 300$ GeV,³⁰ implying the existence of at least one neutralino and one chargino lighter than the squark (sbottom here). Then standard SUSY two-body decays of the squarks are also open, and can be used to set a lower bound on λ' , based on the fact that the BR associated with the lepto-quark channel cannot be very suppressed if such a signal is seen at the LHC.

In Appendix C, we estimate this lower bound on λ'_{i33} for the two final states in (29) without missing energy - (i) charge $\frac{2}{3}$, $l_L^+ b_R$, and (ii) charge $-\frac{1}{3}$, $l_L^- t_R$. For (i), we find $\lambda'_{i33} \gtrsim 0.01 - 0.1$, while for (ii) the lower bounds are slightly smaller. Thus, for the charge $\frac{2}{3}$, $l_L^+ b_R$ final state, we estimate:

$$\begin{aligned} m_{\text{LR}}^2 &\lesssim (0.005 - 0.05) \left(\frac{m_{\bar{b}}}{500 \text{ GeV}} \right)^2 \text{ GeV}^2, \\ A_b - \hat{\mu} \tan \beta &\lesssim (0.002 - 0.02) \left(\frac{m_{\bar{b}}}{500 \text{ GeV}} \right)^2 \text{ GeV}, \end{aligned} \quad (31)$$

while the charge $-\frac{1}{3}$, $l_L^- t_R$ final state could be consistent with a sbottom LR mixing term about two orders of magnitude larger. This implies that barring fine-tuned cancellations, both A_b and $\hat{\mu}$ must be highly suppressed relative to $m_{\bar{b}} \sim M_{\text{SUSY}}$. Furthermore, note that the upper bounds (31) are valid at around the electroweak scale. Now, A_b in particular gets contributions from RG running from all Majorana gaugino masses as well as other A terms according to:

$$\frac{dA_b}{dt} \simeq \frac{1}{16\pi^2} \left\{ \frac{32}{3} g_3^2 M_3 + 6g_2^2 M_2 + \frac{14}{15} g_1^2 M_1 + 2y_t^2 A_t + 12y_b^2 A_b \right\}, \quad (32)$$

where y and A (with appropriate subscripts) are the Yukawa couplings and A -terms,³¹ respectively, while M_i are the $SU(3)_C \times SU(2)_L \times U(1)_Y$ Majorana gaugino masses. Even for a low scale cutoff $\Lambda \sim 10$ TeV, the individual contributions to A_b would be:

$$\Delta A_b \sim \{0.2 M_3, 0.05 M_2, 0.002 M_1\} \text{ GeV}, \quad (\text{from Majorana masses}),$$

²⁹More precisely, the relevant $\hat{\mu}$ -term corresponds to the superpotential bilinear linking the Higgs doublets giving rise to up-type and down-type fermion masses, and is *not* the same as μ in (11). In fact, in R -symmetric models, $\hat{\mu} = 0$.

³⁰ μ is the coefficient of the term $H_u R_d$ in the superpotential in (11).

³¹The trilinear soft terms are defined with one power of the corresponding Yukawa coupling factored out, as is customary in the flavor diagonal case.

$$\Delta A_b \sim \{0.04 A_t, 6 \times 10^{-4} A_b, 4 \times 10^{-5} A_\tau\} \left(\frac{\tan \beta}{3}\right)^2 \text{ GeV}, \quad (\text{from A terms}). \quad (33)$$

The weaker bound in (31) would then imply

$$\begin{aligned} (M_3, M_2, M_1) &\lesssim (0.1, 0.4, 10) \left(\frac{m_{\tilde{b}}}{500 \text{ GeV}}\right)^2 \text{ GeV}, \\ (A_t, A_b, A_\tau) &\lesssim (0.5, 30, 500) \left(\frac{m_{\tilde{b}}}{500 \text{ GeV}}\right)^2 \left(\frac{3}{\tan \beta}\right)^2 \text{ GeV}, \end{aligned} \quad (34)$$

which would become stronger by one order of magnitude if the stronger bound in (31) applies. Thus, in addition to upper bounds on A_b and $\hat{\mu}$ from (31), we also get significant upper bounds on the *three* Majorana gaugino masses as well as on A_t . For larger $\tan \beta$ the bounds are even tighter and one could also infer an upper bound on A_τ as low as a few GeV. Since the absence of Majorana gaugino masses, A -terms, and the $\hat{\mu}$ term are the hallmark of an R -symmetry, the observation of a lepto-quark signal, via a connection to neutrino masses, allows one to build a strong case for the presence of an approximate $U(1)_R$ symmetry at the TeV scale.

7.3.1 Special Cases

As mentioned earlier, there exists special cases in which RPV models can also give rise to visible LQ signals, consistent with neutrino masses and other constraints. First, it may be possible for the LQ to correspond to a second generation squark, e.g. \tilde{c}_L , decaying via the λ'_{123} coupling as $\tilde{c}_L \rightarrow b_R e_L^+$ (and $\tilde{s}_L \rightarrow b_R \bar{\nu}_e$). The point is that such couplings are not constrained by neutrino mass bounds, and the constraints arise from very loose “single coupling bounds”, or from “product coupling bounds” that can allow λ'_{123} to be sizeable if the other coupling is sufficiently suppressed. If couplings like λ'_{123} are indeed sizeable, special kinematic configurations would not be required for the LQ channel to have a visible branching fraction. Nevertheless, observation of a LQ signal is only feasible if the LQ is well below 1 TeV. Thus, given the strong bounds on first two generation squarks in RPV models without an R -symmetry, such an interpretation would require a significant mass splitting between \tilde{c}_L and the other squarks. Such a situation would be distinguishable from the case where the LQ signal arises from third generation squarks. For instance, the “standard” decays of the LQ to the “LSP” (which decays further), for example $\tilde{c}_L \rightarrow c \tilde{\chi}_1^0$ versus $\tilde{t}_L \rightarrow t \tilde{\chi}_1^0$, could distinguish between the two situations.

Thus, we focus on the more natural SUSY interpretation of a LQ signal as a third generation squark, which might still be consistent with a very suppressed λ'_{i33} . This happens when *all other* decay modes of the squarks are suppressed, so that the LQ decay modes have a significant branching fraction even with suppressed λ'_{i33} couplings. Some situations in which this can arise are the following:

- There is only a single LQ signal and it is the LSP. Then *only* LQ decay modes are available, if the LQ is \tilde{b}_R . If the LQ is the doublet, one could hope to use the decay of the heavier into the lighter $SU(2)_L$ component, via an (off-shell) W , to extract additional information. However, besides the 3-body phase space suppression factor, the corresponding partial width scales like $(\Delta m)^5$, where Δm is the splitting between the two $SU(2)$ lepto-quark components. As a result, the derived lower bound on $(\lambda')^2$ is not useful to conclude that the LR mixing should be suppressed.

- The observed LQ is \tilde{b}_R while the doublet LQ's are too heavy, and/or the BR in their LQ channels is too small (so that they are not seen in those channels), and if in addition the LSP neutralino is almost pure wino or almost pure \tilde{H}_u , then the 2-body decay of \tilde{b}_R into the neutralino LSP is highly suppressed. This case could then be similar to the previous one, unless the second-lightest neutralino is lighter than \tilde{b}_R .
- All neutralinos and charginos are heavier than the LQ (or very near threshold), even if the LQ is not the LSP. One then has to compare against loop-induced 2-body decays, or 3-body decays. Such decays are sufficiently suppressed that a sizeable BR in the LQ channel is allowed, consistent with neutrino bounds and without LR suppression.
- Even though the LSP is a neutralino, the LQ happens to be a (highly mixed) stop with the $t\chi^0$ channel kinematically closed. One is then again left with loop-induced 2-body decays, or 3-body decays that can compete against the LQ signal even for rather small λ' [66].

In order to further discriminate between the $U(1)_R$ -symmetry interpretation and the above possibilities, further information regarding the SUSY spectrum would be required. For example, the observation of the prompt decay of the neutralino to say We , which indicates the presence of an appreciable sneutrino vev , could be used to reconstruct the mass of the neutralino as well as shed light into the structure of neutralino interactions, providing support for this class of models over traditional RPV models. A thorough discussion of these issues is left for future work.

7.4 LHC Signals of a Large Sneutrino vev

We have seen in previous subsections that the model produces several distinctive signals at the LHC. Although standard RPV models can give rise to many of these signals in principle, we saw in Sections 7.2 and 7.3 that the full pattern of signals is *generically* different. Furthermore, there is a particular signal topology which clearly distinguishes this model from standard RPV models. Not surprisingly, this difference arises due to the presence of a significant sneutrino vev , which is a distinctive feature of the model.

Such a sneutrino vev opens up the neutralino decay modes into We , $Z\nu$ and $h\nu$. As will be explained in detail in the companion paper [1], these decay modes have sizeable branching fractions when \tilde{X}_1^{0+} is the “LSP”. We therefore focus on this particular situation. The decay mode into We points unambiguously toward a mixing between the electron and the charginos. Although this signal could be interpreted also in the context of a standard RPV model with the left-handed sneutrino acquiring a vev , since the bounds from neutrino masses on the sneutrino vev are so stringent in the standard case, the neutralino typically decays outside the detector or through a displaced vertex. Therefore, a *prompt* decay of the neutralino into We is a clear sign of a sizable sneutrino vev and therefore a hint of a leptonic R -symmetry ($R = R_1$).

Furthermore, even in the case where the decay $\tilde{X}_1^{0+} \rightarrow Z\bar{\nu}_e$ or $h\bar{\nu}_e$ is dominant (with the We channel suppressed, as can happen in some regions of parameter space), the observation of a “mixed topology” signal³² from the pair-production of third generation squarks, could provide a large amount

³²That is, a LQ decay channel on one cascade leg and a “standard” SUSY decay on the other one.

of information. For example if one of the pair-produced \tilde{t}_L 's decays via a LQ channel³³ as in Section 7.3, while the other one decays via $\tilde{t}_L \rightarrow t \tilde{X}_1^{0+} \rightarrow t \{Z\bar{\nu}_e, h\bar{\nu}_e\}$, this could be argued to provide evidence for a leptonic R -symmetry. This is because an observation of such a signal would allow us to draw several conclusions:

- First, there is a neutralino lighter than \tilde{t}_L . In addition, the λ' coupling of the LQ decay channel is large enough to give an observable signal. In particular, one can conclude that the magnitude of λ' is comparable to that of the electroweak gauge couplings.
- The invisible particle is most probably a neutrino. It cannot be a neutralino LSP (in an RPV-MSSM scenario) since it would have decayed promptly through the λ' coupling above into b -quarks and a neutrino (but we are imagining that the Z or h above have been reconstructed). The invisible particle cannot be the gravitino either since the three body decay mode of the neutralino into $b\bar{b}\nu$ via a λ' comparable to electroweak gauge couplings will dominate over the two body decay into $\tilde{G}Z$ or $\tilde{G}h$. For example, for a bino-like NLSP, $\Gamma(\tilde{\chi}_1^0 \rightarrow \tilde{G}Z) = \frac{m_{\tilde{\chi}_1^0}^5}{48\pi m_{3/2}^2 M_{pl}^2} \left(1 - \frac{M_Z^2}{m_{\tilde{\chi}_1^0}^2}\right)^4 \sin^2 \theta_W$, while $\Gamma(\tilde{\chi}_1^0 \rightarrow b\bar{b}\nu) \approx \lambda'^2 g'^2 \frac{7m_{\tilde{\chi}_1^0}^5}{12288 \pi^3 m_b^4}$ where $m_{\tilde{b}}$ is the mass of the (off-shell) sbottom squark. For λ' comparable to electroweak gauge couplings and $m_{\tilde{b}}$ less than a few TeV, the decay width into the gravitino is always suppressed compared to the three body decay.
- Finally, as argued earlier, an observation of the *prompt* decays $\tilde{\chi}_1^0 \rightarrow Z\nu, h\nu$ is strongly disfavored in standard RPV models from bounds on neutrino masses.

Therefore, an observation of the above mixed topology would also strongly point towards a large sneutrino vev , and hence towards a leptonic R -symmetry ($R = R_1$).

7.5 Distinguishing from Other Models

We now briefly discuss how some other popular supersymmetric models can be distinguished from this model. The “classic” and well studied cases of the “constrained MSSM (cMSSM)” and “phenomenological MSSM (pMSSM)” are easy to distinguish from this model. This is because the presence of R -symmetry in both the gauge and matter sectors, implies many signals which are quite different from the cMSSM and pMSSM models, such as:

- (a) Different production rates and decay modes for squarks.
- (b) Dirac gauginos with suppression of SS dileptons signals.
- (c) Resonant slepton/sneutrino production.
- (d) Lepto-quark (LQ) signals.
- (e) Decay of the “LSP” giving rise to fewer channels with \cancel{E}_T , etc.

³³This has a significant branching ratio, especially if λ'_{333} saturates the bounds in Section 5.

The issue of distinguishing GMSB models from this model is more interesting. In “standard” GMSB models (without any R -symmetry), signals (a)-(d) above should still allow us to easily distinguish it from this model. In R -symmetric gauge mediation models (but with the R -symmetry *not* related to lepton number, i.e. $R \neq R_1$), the signals (a) & (b) are the same as in this model. Signals (c) & (d), however, arise from the LQD^c operators which are only present when $R = R_1$; hence signals (c) and (d) can be used to distinguish among the two models.

Signal (e) deserves some more comments. In GMSB, the gravitino is the LSP, hence the NLSP (such as a neutralino or a stau) can decay to the gravitino via $\tilde{\chi}_1^0 \rightarrow Z\tilde{G}$, $h\tilde{G}$ and $\tilde{\tau} \rightarrow \tau\tilde{G}$ [67]. This can resemble *some* of the decays of the “LSP” in our model: $\tilde{X}_1^{0+} \rightarrow Z\tilde{\nu}_e$, $h\tilde{\nu}_e$ and $\tilde{\tau}_L^- \rightarrow \tau_R^-\tilde{\nu}_e$, as explained at the beginning of Section 7. However, within our framework, the decay modes $\tilde{X}_1^{0+} \rightarrow W^-e^+$, $\tilde{\tau}_L^- \rightarrow \bar{t}_L b_R$, etc., can have a non-trivial branching fraction [1], and do not give any \cancel{E}_T when the W ’s decay fully hadronically, thus allowing for a full reconstruction. Therefore, these decays can clearly distinguish our model from GMSB models. Note that the gravitino is, of course, also present within our model, and is also very light. However, due to its suppressed couplings with matter, the branching ratios of the “LSP” to final states with a gravitino are extremely small and can be neglected.³⁴

7.6 The Case “ $B = R$ ”

We briefly mention some phenomenological features of the case $R = R_2$, i.e. in which the baryon number is identified with an R -symmetry. As mentioned earlier, this case has already been studied in [26] and some aspects of the collider phenomenology have been studied in detail in [68].

In these models, the baryonic RPV operators $\lambda''_{ijk} U_i^c D_j^c D_k^c$ are consistent with the R -symmetry. Therefore, the “LSP” decays into jets via the λ'' couplings in this case, giving rise to final states with very small missing energy. Thus, they may naturally evade most of the current LHC bounds, and have generated renewed interest. However, it is important to note that there is a subtlety. In order to evade the bounds, the decay of the “LSP” has to be prompt, which puts a lower bound on the λ'' couplings, $\lambda'' \gtrsim 10^{-5} - 10^{-4}$ [21]. However, the indirect bounds on many of these couplings from neutron-antineutron ($n - \bar{n}$) oscillations are orders of magnitude stronger than this [21]³⁵. Thus, having a large enough coupling requires either a specific flavor ansatz [69], or some other mechanism which relaxes the bounds, for example if R -parity is broken collectively [70].

Identifying the baryon number with an R -symmetry provides an elegant way to evade these bounds (this point was already made in [26]). Indeed, analogous to the $L = R$ case, here the $U^c D^c D^c$ operator is consistent with the R -symmetry which is identified with the baryon number; hence there are no bounds on λ'' couplings from baryon number violating processes like $n - \bar{n}$ oscillations. The baryonic R -symmetry will be broken by the gravitino mass $m_{3/2}$, hence $n - \bar{n}$ oscillations will constrain $m_{3/2}$ depending on the details of R -breaking and mediation. For example, the contribution to $n - \bar{n}$ oscillation

³⁴Note that this is in contrast to standard GMSB models, and even to R -symmetric GMSB models with $R = R_0$, where the *only* available decay mode of the NLSP is to final states with a gravitino.

³⁵This is true if the couplings are “flavor-generic”.

from tree level sbottom/gluino exchange (see Fig. 4) provides an upper bound on λ''_{113} [21]:

$$\lambda''_{113} \lesssim 1 \times \left(\frac{2 \text{ GeV}}{m_{LR}}\right)^2 \left(\frac{2 \text{ GeV}}{M_{\tilde{g}}}\right)^{1/2} \left(\frac{M_3^D}{1 \text{ TeV}}\right) \left(\frac{m_{\tilde{b}}}{500 \text{ GeV}}\right)^4, \quad (35)$$

where $M_{\tilde{g}}$ is the Majorana gluino mass and m_{LR} is the left-right mixing among the sbottom squarks. Thus, an $\mathcal{O}(1)$ λ'' coupling is possible for $M_{\tilde{g}}, m_{LR} \sim \text{few GeV}$. Within generic gravity mediation, this implies $m_{3/2} \sim \text{few GeV}$ while for anomaly mediation $m_{3/2} \sim 100 \text{ GeV}$. If $m_{3/2} > m_{\text{proton}}$, then there is also no constraint from proton decay (to the gravitino, since in that case it would be the lightest baryon!). In Fig. 4 we also show how the $n - \bar{n}$ oscillation process is related to the single resonant production of \tilde{b}_R . Such a diquark signal would formally play the analogous role of the lepto-quark signals in the $L = R$ realization discussed in previous sections. It would be interesting to try to use this feature to infer that the TeV scale Lagrangian does indeed display an approximate R -symmetry, as was done in the $L = R$ case. This is significantly harder here, since the $n - \bar{n}$ constraint is intimately connected to the first generation, while establishing that the jets in a diquark signal are in fact connected to the first rather than the second generation is not quite feasible. Of course, even observing such a resonance is significantly more challenging than observing a LQ signal, especially below the 1 TeV scale (most recent LHC di-jet searches impose cuts above 1 TeV to control the QCD backgrounds). In this sense, a diquark signal arising from the first two generation squarks (which can be heavier consistent with electroweak naturalness), through λ''_{111} or λ''_{112} , can be interesting. However, since the squarks could well lie below 1 TeV in this model, the low mass region should be kept in mind for such searches. This would also apply for third generation squarks decaying into dijets.

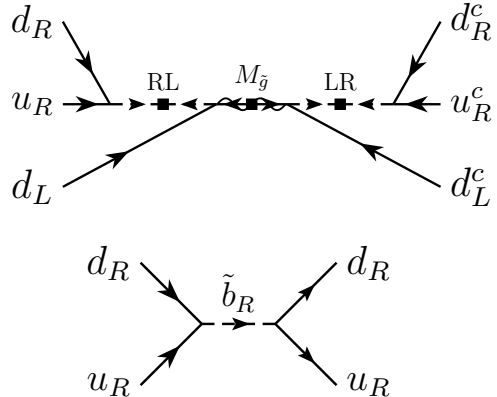


Figure 4: Upper panel: $n - \bar{n}$ oscillations from sbottom exchange via λ''_{113} , showing the Majorana gluino mass and LR insertions (as boxes). The arrows indicate the R number flow. Lower panel: single sbottom resonant production via λ''_{113} .

8 Dark Matter

Since in this class of models the “LSP” decays, there is no WIMP Dark Matter (DM) candidate, similar to generic RPV models. However, other mechanisms for DM generation are available. We leave a detailed exploration of these issues for future work, and only briefly mention a few possibilities.

First, even in the minimal setup considered in this paper, the gravitino can provide a natural DM candidate, as follows. Although we have not studied effects of R -breaking in this paper in detail, such operators are necessarily present, as explained in Appendix A. One of the crucial consequences of these R -breaking operators is the generation of neutrino masses as mentioned earlier. Since the

scale of R -breaking is ultimately tied to $m_{3/2}$, the upper bound on neutrino masses places an upper bound on $m_{3/2}$, the precise magnitude of which depends on the details of R -breaking mediation (see Appendix A for a discussion on two natural possibilities - i) generic gravity mediation, and ii) anomaly mediation). Ref. [25] has studied fitting the entire pattern of experimentally measured neutrino masses and mixing angles within this framework, and finds that $m_{3/2} \lesssim \mathcal{O}(\text{keV})$ for generic gravity mediation, and $m_{3/2} \lesssim \mathcal{O}(1 - 100) \text{ MeV}$ for anomaly mediation. Assuming that the initial gravitino abundance is negligible and is such that it never reaches thermal equilibrium,³⁶ gravitino masses in the keV-MeV range can indeed provide the DM abundance of the Universe by one of the following two processes:

- Thermal scattering of superpartners in the early Universe, as originally explained in [71]. In this case, the gravitino abundance depends linearly on the reheat temperature of the Universe T_R .
- Decays of superpartners, which are still in thermal equilibrium, to gravitinos – also known as *Freeze-in* (FI) [72]. In this case, the gravitino abundance is independent of T_R .

Depending on the superpartner spectrum, one or the other process may dominate or they may both be comparable. Gravitino FI has been studied in [73] (for other discussions of the FI mechanism, see [74–76]). An important point to remember is that since technically the neutrino(s) are the lightest neutralinos in our model (by virtue of lepton number being an R -symmetry, see Section 4.2), the gravitino is *not* absolutely stable. The dominant decay mode of the gravitino \tilde{G} is the process: $\tilde{G} \rightarrow \gamma + \nu$, and it can be shown that the gravitino lifetime is sufficiently long so as to satisfy all observational constraints³⁷ [77].

Finally, it is worth commenting on the tentative γ -line signal at around 130 GeV from the Galactic Center (GC) observed by many groups [78–81] in the FERMI-LAT data. It is clear that if the signal turns out to be correct (confirmed by FERMI-LAT), *and* if it is attributed to DM annihilation, then this cannot be explained within the framework above, at least in its minimal incarnation. Explaining the signal from DM annihilation within this framework would presumably require the existence of an appropriate additional (dark) sector. Studying these issues is left for future work.

9 Conclusions and Future Directions

Without a doubt, we have entered a data-rich era that is expected to finally unravel the mystery of electroweak symmetry breaking, i.e. uncover the physical microscopic mechanism underlying this well-established phenomenon. Although the discovery of a Higgs-like particle near 125 GeV and the absence of new physics so far provides some support for electroweak-tuned theories, it is still rather premature to abandon electroweak-naturalness. Indeed, Nature could be cleverly realizing an electroweak-natural model which manifests itself at the LHC in non-standard ways. In this work, we have studied one such elegant model, the defining feature of which is the existence of a continuous R -symmetry, *that coincides with lepton number when restricted to the SM sector. An important consequence of this is*

³⁶These conditions can be easily satisfied since the gravitino has extremely suppressed couplings.

³⁷We disagree with earlier results for the decay width of the process $\tilde{G} \rightarrow \gamma + \nu$. We believe this discrepancy arises due to the earlier works not taking into account gauge invariance properly, in particular due to effectively using a *non-gauge-invariant* regulator.

that one of the left-handed sneutrinos gets a significant vev , which is not constrained by the upper bound on neutrino masses (we take the sneutrino getting a vev to be of the electron type, so that the corresponding charged lepton can easily get a mass from suppressed operators, while various other constraints are also satisfied). As a result, a large region of parameter space of the model is still viable, and leads to a rather rich and interesting phenomenology.

The most important features of such a framework include i) “Dirac” gauginos (especially gluinos) due to “ R -symmetry in the gauge sector”, ii) Absence of certain scalar trilinear terms and the “standard” μ -parameter (that we have called $\hat{\mu}$ in this work) due to the “ R -symmetry in the matter sector”, iii) Existence of RPV operators of the type $\lambda_{ijk}L_iL_jE_k^c$, $\lambda'_{ijk}L_iQ_jD_k^c$ and $B\mu_L^{(i)}H_uL_i$ consistent with the leptonic R -symmetry $R = R_1$. Due to a significant sneutrino vev , the sneutrino acts as a Higgs field providing the down-type fermion masses through subsets of these operators, iv) Mixing between neutralinos and neutrinos, and between charginos and charged leptons. These features combine to give a rich and complex pattern of signals at the LHC, which is studied in a companion paper [1]. Although subsets of these features are shared by other models, the entire pattern of signals is rather unique and should be distinguishable from other models. Here we have highlighted how the (perhaps imminent) observation of lepto-quark signals could be construed as a powerful indication that the TeV scale Lagrangian indeed displays an approximate $U(1)_R$ symmetry of the leptonic type. We have also discussed how certain topologies at the LHC could be used to infer that the sneutrino vev is non-vanishing (and large), and also that a missing energy observation should be interpreted as being associated with a neutrino (as opposed to a neutralino or a gravitino). Further exploration of these issues will certainly be welcome in the near future.

We emphasize that these models can easily accommodate the observed ~ 125 GeV Higgs-like signal with significantly less tuning than in the MSSM. The main ingredient is the existence of a scalar triplet which must be somewhat heavy ($\gtrsim 1$ TeV), as required by current constraints on the ρ -parameter. If such a triplet scalar has an order one coupling to the Higgs, it can contribute significantly to the Higgs mass at the loop level (the R -symmetry forbids other tree-level contributions). This is similar in spirit to using the stops for such effect within the MSSM, but with significantly less tuning than in that well-known case. This observation is more general than the particular model we are considering, but it fits rather nicely within the $U(1)_R$ framework.

Finally, from the theoretical point of view, it would be very interesting to find a simple *dynamical* mechanism of supersymmetry breaking and mediation which preserves an approximate $U(1)_R$ symmetry, followed by an R -symmetry breaking and mediation mechanism, which generates the structure of operators as envisioned in this class of models.

Acknowledgments

C.F. and T.G. are supported in part by the Natural Sciences and Engineering Research Council of Canada (NSERC). E.P. is supported by the DOE grant DE-FG02-92ER40699. P.K. has been supported by the DOE grant DE-FG02-92ER40699 and the DOE grant DE-FG02-92ER40704 during the course of this work.

A R -breaking Operators

As explained in Section 2.2, there are two natural ways in which R -breaking can be transmitted to the visible sector: i) generic gravity-mediation, and ii) anomaly-mediation.

Starting with generic gravity-mediation, we write *arbitrary Planck suppressed* couplings that are restricted only by the SM gauge symmetries, but which do not respect the (anomalous) $U(1)_R$ symmetry (for concreteness, here we consider the case $R = R_1$). Nevertheless, we assume that $M_\star \ll M_P$, so that the $U(1)_R$ symmetry is approximate in the observable sector, being dominated by the physics at M_\star . Thus, we have $U(1)_R$ -violating superpotential terms:

$$W_{\mathcal{R}} = \hat{\mu} H_u H_d + \mu'_i H_u L_i + \frac{1}{2} M_S S^2 + \frac{1}{2} M_T T^2 + \frac{1}{2} M_O O^2 + \tilde{y}_{ij}^d H_d Q_i D_j^c + \tilde{y}_{ij}^e H_d L_i E_j^c + \frac{1}{3} y_S S^3, \quad (36)$$

which can schematically arise from

$$\int d^4\theta \frac{X^\dagger}{M_P} \left\{ H_u H_d + H_u L_i + S^2 + T^2 + O^2 + \frac{1}{M_P} (H_d Q_i D_j^c + H_d L_i E_j^c + S^3) \right\}. \quad (37)$$

We see that $\mu'_i \sim F_X/M_P \sim m_{3/2}$. In this case, we also see that the contribution to the “standard” (but $U(1)_R$ -violating) down-type and lepton Yukawa couplings is $\tilde{y}_{ij}^d \sim \tilde{y}_{ij}^e \sim m_{3/2}/M_P < 10^{-22}$ for $m_{3/2} \lesssim \text{MeV}$. A similar suppression can be expected for the $U^c D^c D^c$ superpotential operator and other R -violating trilinears. There are also $U(1)_R$ -violating soft-breaking terms:

$$V_{\mathcal{R}}^{\text{soft}} = B\mu_R H_u R_d + A_{ij}^u H_u Q_i U_j^c + A_{ij}^d H_d Q_i D_j^c + A_{ij}^e H_d L_i E_j^c + \tilde{A}_{ijk}^d L_i Q_j D_k^c + \tilde{A}_{ijk}^e L_i L_j E_k^c, \quad (38)$$

which can arise from

$$\int d^4\theta \frac{X^\dagger X}{M_P^2} \left\{ H_u R_d + \frac{1}{M_P} [H_u Q_i U_j^c + \dots] \right\}, \quad (39)$$

giving contributions to the b -terms of order $m_{3/2}^2$, and very suppressed contributions to the A -terms, of order $(m_{3/2}/M_P) m_{3/2}$. However, there are also terms of the form

$$\int d^2\theta \frac{X}{M_P} [H_u Q_i U_j^c + \dots], \quad (40)$$

that give contributions to the A -terms of order $m_{3/2}$. Again, we consider only Planck suppressed couplings between the hidden and observable fields, so that no $\int d^2\theta X H_u H_d$ operator, which would induce a too large $B\mu_R$ term, exists. Similarly, there can exist $U(1)_R$ -violating gaugino Majorana masses $\frac{1}{2} M_a \lambda^a \lambda^a$, induced by

$$\frac{1}{2} \int d^2\theta \frac{X}{M_P} \mathcal{W}^\alpha \mathcal{W}_\alpha + \text{h.c.} \quad (41)$$

so that $M_a \sim m_{3/2}$. Thus, the scale of $U(1)_R$ -preserving terms is taken to be M_{SUSY} , which is assumed to be much larger than the scale of $U(1)_R$ -violating operators, set by $m_{3/2}$. All possible dimensionful

terms allowed by the gauge symmetries are allowed, and are induced at least at order $m_{3/2}$. Note that singlets in theories of the present type have been argued to be safe from radiatively-induced tadpoles [46]. Finally, as mentioned in the main text, the experimental upper bound on neutrino masses puts an upper bound on $m_{3/2}$ in this case to be $\mathcal{O}(\text{keV})$ [25].

In the case of anomaly-mediation, we imagine a situation in which the “tree-level” transmission of R -breaking by operators (37), (39), (40) and (41) is very suppressed, e.g. due to sequestering. Then anomaly-mediation generates essentially the same operators (40) and (41), except that they are generated at one-loop rather than at tree-level. So, the coefficients above are suppressed by the one-loop factor $\sim \frac{1}{16\pi^2}$, giving rise to an associated mass scale:

$$M_a^{\text{anomaly}}, A^{\text{anomaly}} \sim \frac{m_{3/2}}{16\pi^2}. \quad (42)$$

In this case, the upper bound on $m_{3/2}$ from the neutrino mass constraint is $\mathcal{O}(1 - 100) \text{ MeV}$ [25].

B A Flavor Ansatz

In Section 5.2, we saw that there exist a number of constraints on the λ and λ' couplings from various flavor-violating processes. In Section 7, we also studied phenomenological consequences of an ansatz in which all the λ and λ' couplings are assumed to saturate the bounds in Tables 3, 4 and 5 (except λ'_{311} , which is taken to be negligible.). However, it is also possible to consider other simple ansätze about the flavor dependence of these couplings, and we discuss such an option here which allows a nice understanding of the relative magnitudes of the various couplings and also satisfies existing constraints. Also, it has the advantage of *further* reducing the number of independent λ and λ' couplings.

We imagine that the model described by the superpotential in (11) has a flavor symmetry $G_F \equiv SU(3)_Q \times SU(3)_U \times SU(3)_D \times SU(3)_L \times SU(3)_E$ at some high scale which is broken by scalar components of “flavon” superfields. This implies that the up-type Yukawa couplings and the λ and λ' couplings (which include down-type and lepton Yukawa couplings) should be thought of as flavon (super) fields transforming in a non-trivial representation of G_F . Of course, the symmetry group G_F is broken when their scalar components get *vev*’s and give rise to the numerical values of the Yukawa couplings. The representations in Table 7 allow all the relevant operators in the superpotential in (11).

In particular, the above choice gives rise to the following structure for the coefficient of $L_i L_j E_k^c$:³⁸

$$\lambda^{ijk} = \epsilon^{ijn} Y_n^k, \quad (43)$$

where ϵ^{ijk} stands for the antisymmetric tensor with three indices, and Y_n^k transforms in the $(\square, \bar{\square})$ of $SU(3)_L \times SU(3)_E$. Then, using the $SU(3)_L$ and $SU(3)_E$ rotation freedoms for L_j and E_k^c , respectively,

³⁸In this section only, we use subscripts (superscripts) to denote transformation in the fundamental (anti-fundamental) of $SU(3)$.

	$SU(3)_Q$	$SU(3)_U$	$SU(3)_D$	$SU(3)_L$	$SU(3)_E$
Q	\square	1	1	1	1
U^c	1	\square	1	1	1
D^c	1	1	\square	1	1
L	1	1	1	\square	1
E^c	1	1	1	1	\square
Y_u	$\bar{\square}$	$\bar{\square}$	1	1	1
λ'	$\bar{\square}$	1	$\bar{\square}$	$\bar{\square}$	1
λ	1	1	1	$\square\square$	$\bar{\square}$

Table 7: Representations of the fields and Yukawa spurions under G_F .

it is possible to choose a convenient form of Y_n^k . In particular, by choosing:³⁹

$$\begin{aligned}
Y_n^k &= y_1 \delta_n^k, & n = 1, \\
&= -y_3 \delta_3^k, & n = 2, \\
&= y_2 \delta_2^k, & n = 3,
\end{aligned} \tag{44}$$

one gets a simple structure of the λ_{ijk} couplings, in which the matrix λ_{1jk} is a diagonal matrix corresponding to the usual leptonic Yukawa couplings appearing in W_{Yukawa} in Eq. (15) with $y_2 = y_2^{(e)} \equiv y_\mu$, and $y_3 = y_3^{(e)} \equiv y_\tau$.⁴⁰ Furthermore, the matrices λ_{2jk} and λ_{3jk} have only one independent λ_{ijk} coupling: $\lambda_{231} = -\lambda_{321} = y_1$; the rest either vanish or are related to the previous Yukawa couplings.

The LQD^c operators are less constrained by these arguments. However, it is convenient to make the following simple ansatz:

$$(\lambda')^{ijk} \sim y_i (\hat{Y}_d)^{jk}, \tag{45}$$

where y_i are defined in (44), and $(\hat{Y}_d)^{jk}$ transforming in the $(\bar{\square}, \bar{\square})$ of $SU(3)_Q \times SU(3)_D$. Again, by choosing an appropriate $SU(3)_Q \times SU(3)_D$ rotation, $(\hat{Y}_d)^{jk}$ can be brought into the form $\text{diag}(\hat{y}_1, \hat{y}_2, \hat{y}_3)$, which results in a very simple structure of the λ'_{ijk} couplings as well. In particular, the matrix λ'_{1jk} is diagonal and corresponds to the usual down-type quark Yukawa couplings in W_{Yukawa} in (15). The remaining λ' couplings are *completely* fixed by these down-type Yukawa couplings and the numbers $\{y_1, y_2, y_3\}$ in (44). Since y_2 and y_3 are the muon and tau Yukawa couplings, the only other independent input to fix all the remaining ones is $y_1 = \lambda_{231} = -\lambda_{321}$.

Since the above ansatz provides a concrete determination of all the couplings, it is straightforward (but tedious) to check constraints from all combinations of λ and λ' couplings in [21, 51–53]. We find that all such constraints are readily satisfied, except that coming from $|\lambda_{231} \lambda'_{311}|$, which is violated by a small amount. This, however, just means that (45) is only approximate and receives some corrections. In any case, the main motivation for the ansatz (45) is to simplify the structure of the λ' couplings,

³⁹This can be achieved by diagonalizing Y_n^k by bi-unitary transformations, followed by the exchange of the second and third rows, with an appropriate sign.

⁴⁰Note the electron mass arises not from superpotential couplings, but from SUSY breaking operators; see Section 4.

and perhaps suggest a possible high-energy rationale for their structure.

Finally, since the only new coupling within this approach is y_1 , it is important to know what one would generically expect for its size. In fact, the bound on the product $|\lambda'_{133} \lambda'_{233}| \equiv y_b |\lambda'_{233}| < 1.1 \times 10^{-5}$ [53] puts a bound on y_1 , since in our framework $y_b \lambda'_{233} \simeq \frac{y_\mu y_b^2}{y_1} \simeq (1.53 \times 10^{-7} \text{ sec}^3 \beta)/y_1$. Therefore, the bound implies that the *largest* non-Yukawa λ' coupling (λ'_{333}) is roughly given by:

$$\lambda'_{333} \sim \frac{y_\tau y_b}{y_1} \lesssim 0.011 \cos \beta, \quad (46)$$

which is quite small. However, this bound is specific to the previous ansatz and, experimentally, λ'_{333} can be significantly larger, as described in the main text (where we do not use the ansatz of this section). We still describe it here as it is simple and will also be considered in our LHC phenomenology study in [1].

C Lower Bound on λ'_{i33} given the Observation of an LQ Signal

In this appendix we argue that typically the size of the relevant λ' couplings cannot be extremely suppressed, if a LQ signal was observed at the LHC. In order to estimate a *lower* bound on $(\lambda')^2$ such that the BR in the LQ channel is not very suppressed (and could be observed in the near future), we explore several possibilities, depending on whether the lepto-quark is \tilde{t}_L , \tilde{b}_L or \tilde{b}_R . To be definite we estimate the “minimum” value of $(\lambda')^2$ by requiring that the partial decay width in the lepto-quark channel, given by $\Gamma_{\text{LQ}} = [(\lambda')^2/16\pi] m_{\text{LQ}}$ equals one of the standard R-parity conserving 2-body decay widths [82], $\Gamma_{2\text{-body}}$, interpreted within the MSSM:⁴¹

$$(\lambda'_{\text{min}})^2 \equiv \frac{16\pi}{m_{\text{LQ}}} \Gamma_{2\text{-body}}. \quad (47)$$

We show in Fig. 5 the result for 500 GeV lepto-quarks, when comparing to their partial decay widths into a neutralino plus quark (left column) and into a chargino plus quark (middle column). We have performed a scan over $M_1, M_2, |\mu| \in [0, 600]$ GeV and $\tan \beta \in [3, 50]$, diagonalizing the MSSM neutralino and chargino mass matrices to find the spectrum and composition of the eigenstates for each parameter point. We compare to the *dominant* neutralino or chargino channel, and plot the $(\lambda'_{\text{min}})^2$ defined above, as a function of $\Delta m = m_{\text{LQ}} - m_\chi$, where $m_{\text{LQ}} = 500$ GeV is the lepto-quark mass and m_χ is the appropriate neutralino or chargino mass. We also show curves corresponding to the limiting cases in which the neutralino is pure bino, pure wino or pure Higgsino (\tilde{h}_u), and also when the chargino is pure gaugino or pure Higgsino. For each scanned parameter point we have also estimated $(\lambda'_{\text{min}})^2$ based on the *largest* partial decay width of *any* of the neutralino *and* chargino channels (shown in the right column plots). We will use the latter as our estimate for $(\lambda'_{\text{min}})^2$.

We see from the plots in the right column that in the case that the lepto-quark is a $SU(2)_L$ doublet, $(\lambda'_{\text{min}})^2$ is typically above 0.01 (unless the decay is very close to threshold). We also note that

⁴¹We show the results within the MSSM structure to illustrate what an interpretation outside the $U(1)_R$ symmetric framework would entail. A similar analysis within the $L = R$ model results in qualitatively similar features regarding the expected sizes of the λ' couplings.

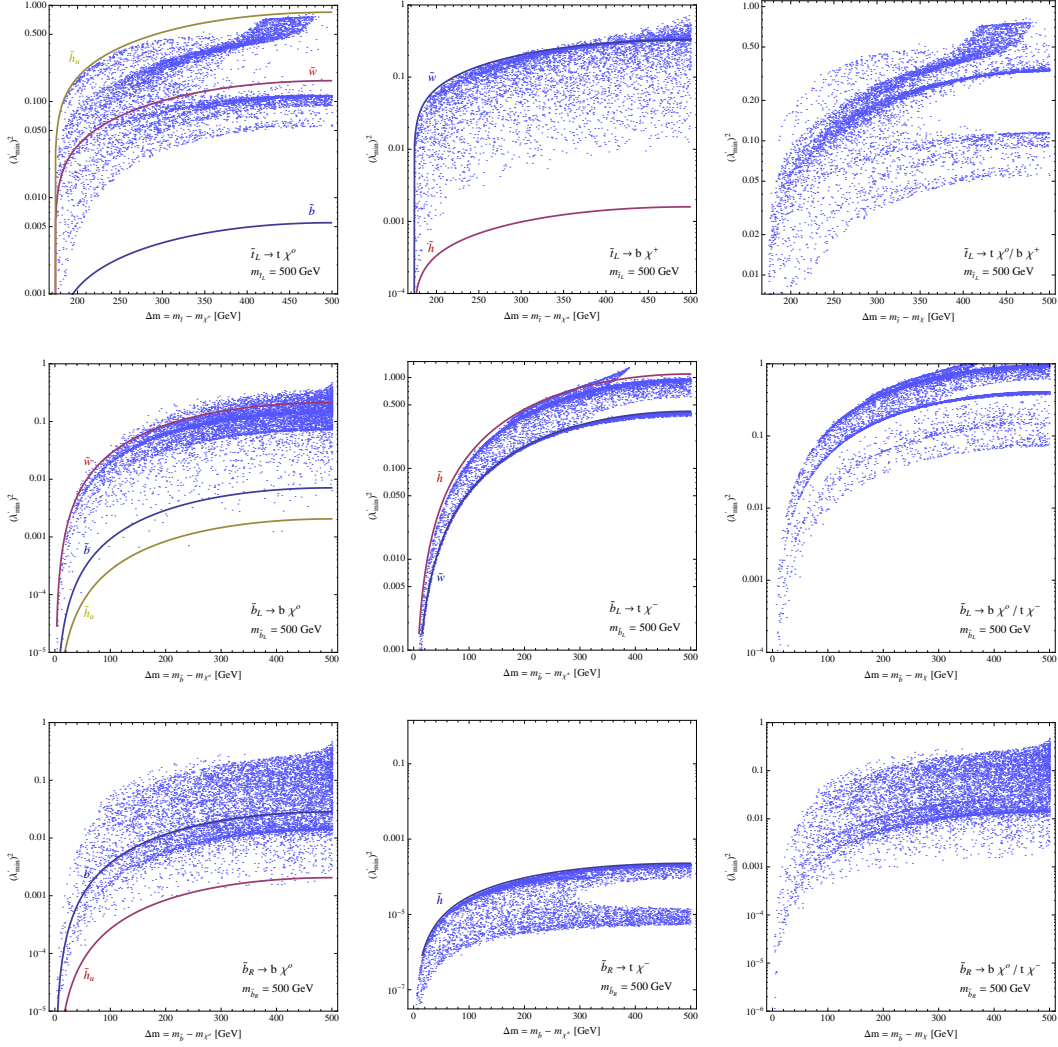


Figure 5: Required value of $(\lambda')^2$ such that the partial width in the lepto-quark signal equals the standard 2-body decay width into neutralinos/charginos for a 500 GeV \tilde{t}_L (upper row), \tilde{b}_L (middle row) and \tilde{b}_R (lower row), within the RPV-MSSM. The third column uses the largest of the neutralino/chargino channels to bound $(\lambda')^2$ for any given point in the random scan over M_1, M_2, μ and $\tan\beta$. The smooth curves indicate the limit where the neutralino is pure bino, pure wino and pure higgsino, as indicated, and similarly for the chargino being pure wino or higgsino.

the bulk of the cases has an even larger $(\lambda'_{\min})^2 \gtrsim 0.1$. Our estimate given in (31) is obtained by using $(\lambda'_{\min})^2 \sim 0.01 - 0.1$ in (30), together with $\Delta m_\nu \sim 0.1$ eV. We also see from the lower row in Fig. 5 that when the lepto-quark is \tilde{b}_R , our estimate for $(\lambda'_{\min})^2$ is weaker, although still larger than what the neutrino bound requires if there was no suppression from LR mixing in the sbottom sector. These two cases could be distinguished by the type of lepto-quark signal: bl for the doublet (we expect the mass splitting between \tilde{t}_L and \tilde{b}_L to not exceed a few tens of GeV), and tl for the singlet. Both cases should be accompanied by a $b + \cancel{E}_T$ signal, that would suggest that the missing energy comes from a neutrino.

References

- [1] C. Frugiuele, T. Grégoire, P. Kumar, and E. Pontón, ““ $L=R$ ” - $U(1)_R$ Lepton Number at the LHC,” arXiv:1208.xxxx [hep-ph].
- [2] **CMS Collaboration** Collaboration, S. Chatrchyan *et al.* *Phys.Lett.* **B716** (2012) 30–61, arXiv:1207.7235 [hep-ex].
- [3] **ATLAS Collaboration** Collaboration, G. Aad *et al.* *Phys.Lett.* **B716** (2012) 1–29, arXiv:1207.7214 [hep-ex].
- [4] J. D. Wells *Phys.Rev.* **D71** (2005) 015013, arXiv:hep-ph/0411041 [hep-ph].
- [5] N. Arkani-Hamed and S. Dimopoulos *JHEP* **0506** (2005) 073, arXiv:hep-th/0405159 [hep-th].
- [6] B. S. Acharya, K. Bobkov, G. L. Kane, P. Kumar, and J. Shao *Phys.Rev.* **D76** (2007) 126010, arXiv:hep-th/0701034 [hep-th].
- [7] B. S. Acharya, K. Bobkov, G. L. Kane, J. Shao, and P. Kumar *Phys.Rev.* **D78** (2008) 065038, arXiv:0801.0478 [hep-ph].
- [8] G. Kane, P. Kumar, R. Lu, and B. Zheng *Phys.Rev.* **D85** (2012) 075026, arXiv:1112.1059 [hep-ph].
- [9] A. G. Cohen, D. Kaplan, and A. Nelson *Phys.Lett.* **B388** (1996) 588–598, arXiv:hep-ph/9607394 [hep-ph].
- [10] R. Sundrum *JHEP* **1101** (2011) 062, arXiv:0909.5430 [hep-th].
- [11] T. Gherghetta, B. von Harling, and N. Setzer *JHEP* **1107** (2011) 011, arXiv:1104.3171 [hep-ph].
- [12] C. Csaki, L. Randall, and J. Terning arXiv:1201.1293 [hep-ph].
- [13] G. Larsen, Y. Nomura, and H. L. Roberts *JHEP* **1206** (2012) 032, arXiv:1202.6339 [hep-ph].
- [14] T. Cohen, A. Hook, and G. Torroba arXiv:1204.1337 [hep-ph].
- [15] N. Craig, M. McCullough, and J. Thaler *JHEP* **1206** (2012) 046, arXiv:1203.1622 [hep-ph].
- [16] T. J. LeCompte and S. P. Martin *Phys.Rev.* **D85** (2012) 035023, arXiv:1111.6897 [hep-ph].
- [17] T. J. LeCompte and S. P. Martin *Phys.Rev.* **D84** (2011) 015004, arXiv:1105.4304 [hep-ph].
- [18] H. Murayama, Y. Nomura, S. Shirai, and K. Tobioka arXiv:1206.4993 [hep-ph].
- [19] J. Fan, M. Reece, and J. T. Ruderman *JHEP* **1111** (2011) 012, arXiv:1105.5135 [hep-ph].

- [20] J. Fan, M. Reece, and J. T. Ruderman [arXiv:1201.4875 \[hep-ph\]](#).
- [21] R. Barbier, C. Berat, M. Besancon, M. Chemtob, A. Deandrea, *et al.* *Phys.Rept.* **420** (2005) 1–202, [arXiv:hep-ph/0406039 \[hep-ph\]](#).
- [22] G. D. Kribs and A. Martin [arXiv:1203.4821 \[hep-ph\]](#).
- [23] M. Heikinheimo, M. Kellerstein, and V. Sanz *JHEP* **1204** (2012) 043, [arXiv:1111.4322 \[hep-ph\]](#).
- [24] C. Frugiuale and T. Grégoire *Phys.Rev.* **D85** (2012) 015016, [arXiv:1107.4634 \[hep-ph\]](#).
- [25] E. Bertuzzo and C. Frugiuale *JHEP* **1205** (2012) 100, [arXiv:1203.5340 \[hep-ph\]](#).
- [26] C. Brust, A. Katz, S. Lawrence, and R. Sundrum *JHEP* **1203** (2012) 103, [arXiv:1110.6670 \[hep-ph\]](#).
- [27] C. Csaki, Y. Grossman, and B. Heidenreich *Phys.Rev.* **D85** (2012) 095009, [arXiv:1111.1239 \[hep-ph\]](#).
- [28] P. J. Fox, A. E. Nelson, and N. Weiner *JHEP* **0208** (2002) 035, [arXiv:hep-ph/0206096 \[hep-ph\]](#).
- [29] G. D. Kribs, E. Poppitz, and N. Weiner *Phys.Rev.* **D78** (2008) 055010, [arXiv:0712.2039 \[hep-ph\]](#).
- [30] L. J. Hall *Mod.Phys.Lett.* **A5** (1990) 467.
- [31] L. Hall and L. Randall *Nucl.Phys.* **B352** (1991) 289–308.
- [32] A. E. Nelson, N. Rius, V. Sanz, and M. Unsal *JHEP* **0208** (2002) 039, [arXiv:hep-ph/0206102 \[hep-ph\]](#).
- [33] Z. Chacko, P. J. Fox, and H. Murayama *Nucl.Phys.* **B706** (2005) 53–70, [arXiv:hep-ph/0406142 \[hep-ph\]](#).
- [34] K. Benakli and M. Goodsell *Nucl.Phys.* **B816** (2009) 185–203, [arXiv:0811.4409 \[hep-ph\]](#).
- [35] S. Choi, M. Drees, A. Freitas, and P. Zerwas *Phys.Rev.* **D78** (2008) 095007, [arXiv:0808.2410 \[hep-ph\]](#).
- [36] A. Kumar, D. Tucker-Smith, and N. Weiner *JHEP* **1009** (2010) 111, [arXiv:0910.2475 \[hep-ph\]](#).
- [37] B. A. Dobrescu and P. J. Fox *Eur.Phys.J.* **C70** (2010) 263–270, [arXiv:1001.3147 \[hep-ph\]](#).
- [38] K. Benakli *Fortsch.Phys.* **59** (2011) 1079–1082, [arXiv:1106.1649 \[hep-ph\]](#).
- [39] R. Davies and M. McCullough *Phys.Rev.* **D86** (2012) 025014, [arXiv:1111.2361 \[hep-ph\]](#).

- [40] K. Benakli and M. Goodsell *Nucl.Phys.* **B840** (2010) 1–28, arXiv:1003.4957 [hep-ph].
- [41] S. Abel and M. Goodsell *JHEP* **1106** (2011) 064, arXiv:1102.0014 [hep-th].
- [42] P. Kumar and E. Pontón *JHEP* **1111** (2011) 037, arXiv:1107.1719 [hep-ph].
- [43] R. Fok, G. D. Kribs, A. Martin, and Y. Tsai arXiv:1208.2784 [hep-ph].
- [44] A. E. Nelson and N. Seiberg *Nucl.Phys.* **B416** (1994) 46–62, arXiv:hep-ph/9309299 [hep-ph].
- [45] N. Arkani-Hamed, S. Dimopoulos, G. Giudice, and A. Romanino *Nucl.Phys.* **B709** (2005) 3–46, arXiv:hep-ph/0409232 [hep-ph].
- [46] M. D. Goodsell arXiv:1206.6697 [hep-ph].
- [47] G. D. Kribs, T. Okui, and T. S. Roy *Phys.Rev.* **D82** (2010) 115010, arXiv:1008.1798 [hep-ph].
- [48] R. Davies, J. March-Russell, and M. McCullough *JHEP* **1104** (2011) 108, arXiv:1103.1647 [hep-ph].
- [49] R. Fok and G. D. Kribs *Phys.Rev.* **D82** (2010) 035010, arXiv:1004.0556 [hep-ph].
- [50] W. Loinaz, N. Okamura, S. Rayyan, T. Takeuchi, and L. Wijewardhana *Phys.Rev.* **D70** (2004) 113004, arXiv:hep-ph/0403306 [hep-ph].
- [51] J. P. Saha and A. Kundu *Phys.Rev.* **D66** (2002) 054021, arXiv:hep-ph/0205046 [hep-ph].
- [52] H. Dreiner, M. Kramer, and B. O’Leary *Phys.Rev.* **D75** (2007) 114016, arXiv:hep-ph/0612278 [hep-ph].
- [53] H. Dreiner, K. Nickel, F. Staub, and A. Vicente *Phys.Rev.* **D86** (2012) 015003, arXiv:1204.5925 [hep-ph].
- [54] E. Bertuzzo, C. Frugiuele, T. Grégoire, P. Kumar, and E. Pontón, “To appear,”.
- [55] **Particle Data Group** Collaboration, C. Amsler *et al.* *Phys.Lett.* **B667** (2008) 1–1340.
- [56] G. Belanger, K. Benakli, M. Goodsell, C. Moura, and A. Pukhov *JCAP* **0908** (2009) 027, arXiv:0905.1043 [hep-ph].
- [57] K. Benakli, M. D. Goodsell, and A.-K. Maier *Nucl.Phys.* **B851** (2011) 445–461, arXiv:1104.2695 [hep-ph].
- [58] J. R. Espinosa, C. Grojean, V. Sanz, and M. Trott arXiv:1207.7355 [hep-ph].
- [59] F. Staub, “SARAH,” arXiv:0806.0538 [hep-ph].
- [60] F. Staub *Comput.Phys.Commun.* **182** (2011) 808–833, arXiv:1002.0840 [hep-ph].

- [61] **CMS Collaboration** Collaboration CMS-PAS-SUS-11-016.
- [62] **ATLAS Collaboration** Collaboration, G. Aad *et al.* *JHEP* **1207** (2012) 167, arXiv:1206.1760 [hep-ex].
- [63] **CMS Collaboration** Collaboration, “<https://twiki.cern.ch/twiki/bin/view/CMSPublic/SUSYSMSSummaryPlots>,”.
- [64] **ATLAS Collaboration** Collaboration, P. Jackson arXiv:1112.0369 [hep-ex].
- [65] **ATLAS Collaboration** Collaboration, G. Aad *et al.* *Phys.Rev.Lett.* **107** (2011) 272002, arXiv:1108.1582 [hep-ex].
- [66] S. P. Das, A. Datta, and S. Poddar *Phys.Rev.* **D73** (2006) 075014, arXiv:hep-ph/0509171 [hep-ph].
- [67] Y. Kats, P. Meade, M. Reece, and D. Shih *JHEP* **1202** (2012) 115, arXiv:1110.6444 [hep-ph].
- [68] C. Brust, A. Katz, and R. Sundrum arXiv:1206.2353 [hep-ph].
- [69] G. D’Ambrosio, G. Giudice, G. Isidori, and A. Strumia *Nucl.Phys.* **B645** (2002) 155–187, arXiv:hep-ph/0207036 [hep-ph].
- [70] J. T. Ruderman, T. R. Slatyer, and N. Weiner arXiv:1207.5787 [hep-ph].
- [71] T. Moroi, H. Murayama, and M. Yamaguchi *Phys.Lett.* **B303** (1993) 289–294.
- [72] L. J. Hall, K. Jedamzik, J. March-Russell, and S. M. West *JHEP* **1003** (2010) 080, arXiv:0911.1120 [hep-ph].
- [73] C. Cheung, G. Elor, and L. Hall *Phys.Rev.* **D84** (2011) 115021, arXiv:1103.4394 [hep-ph].
- [74] C. Cheung, G. Elor, L. J. Hall, and P. Kumar *JHEP* **1103** (2011) 042, arXiv:1010.0022 [hep-ph].
- [75] C. Cheung, G. Elor, L. J. Hall, and P. Kumar *JHEP* **1103** (2011) 085, arXiv:1010.0024 [hep-ph].
- [76] L. J. Hall, J. March-Russell, and S. M. West arXiv:1010.0245 [hep-ph].
- [77] T. Grégoire and E. Pontón, “To appear,”.
- [78] T. Bringmann, X. Huang, A. Ibarra, S. Vogl, and C. Weniger *JCAP* **1207** (2012) 054, arXiv:1203.1312 [hep-ph].
- [79] C. Weniger arXiv:1204.2797 [hep-ph].
- [80] E. Tempel, A. Hektor, and M. Raidal *JCAP* **1209** (2012) 032, arXiv:1205.1045 [hep-ph].
- [81] M. Su and D. P. Finkbeiner arXiv:1206.1616 [astro-ph.HE].
- [82] A. Djouadi and Y. Mambrini *Phys.Rev.* **D63** (2001) 115005, arXiv:hep-ph/0011364 [hep-ph].